

1 Effects of Emission Reductions on Organic Aerosol in 2 the Southeastern United States

3
4 C. L. Blanchard¹, G. M. Hidy², S. Shaw³, K. Baumann⁴, E. S. Edgerton⁴

5 [1] Envair, Albany, CA, USA

6 [2] Envair/Aerochem, Placitas, NM, USA

7 [3] Environmental Sector, Electric Power Research Institute, Palo Alto, CA, USA

8 [4] Atmospheric Research and Analysis, Cary, NC, USA

9 Correspondence to: C. L. Blanchard (cbenvair@pacbell.net)

10 11 Abstract

12 Long-term (1999 to 2013) data from the Southeastern Aerosol Research and
13 Characterization (SEARCH) network are used to show that anthropogenic emission
14 reductions led to important decreases in fine particle organic aerosol (OA) concentrations
15 in the southeastern U.S. On average, 45% (range 25 to 63%) of the 1999 to 2013 mean
16 organic carbon (OC) concentrations are attributed to combustion processes, including
17 fossil fuel use and biomass burning, through associations of measured OC with
18 combustion products such as elemental carbon (EC), carbon monoxide (CO), and
19 nitrogen oxides (NO_x). The 2013 mean combustion-derived OC concentrations were 0.5
20 to 1.4 μg m⁻³ at the five sites operating in that year. Mean annual combustion-derived OC
21 concentrations declined from 3.8 ± 0.2 μg m⁻³ (68% of total OC) to 1.4 ± 0.1 μg m⁻³
22 (60% of total OC) between 1999 and 2013 at the urban Atlanta, Georgia, site (JST) and
23 from 2.9 ± 0.4 μg m⁻³ (39% of total OC) to 0.7 ± 0.1 μg m⁻³ (30% of total OC) between
24 2001 and 2013 at the urban Birmingham, Alabama, site (BHM). The urban OC declines
25 coincide with reductions of motor vehicle emissions between 2006 and 2010, which may
26 have decreased mean OC concentrations at the urban SEARCH sites by > 2 μg m⁻³. BHM
27 additionally exhibits a decline in OC associated with SO₂ from 0.4 ± 0.04 μg m⁻³ in 2001
28 to 0.2 ± 0.03 μg m⁻³ in 2013, interpreted as the result of reduced emissions from

29 industrial sources within the city. Analyses using non-soil potassium as a biomass
30 burning tracer indicate that biomass burning OC occurs throughout the year at all sites.
31 All eight SEARCH sites show an association of OC with sulfate (SO_4) ranging from 0.3
32 to $1.0 \mu\text{g m}^{-3}$ on average, representing ~25% of the 1999 to 2013 mean OC
33 concentrations. Because the mass of OC identified with SO_4 averages 20 to 30% of the
34 SO_4 concentrations, the mean SO_4 -associated OC declined by ~0.5 to $1 \mu\text{g m}^{-3}$ as SO_4
35 concentrations decreased throughout the SEARCH region. The 2013 mean SO_4
36 concentrations of 1.7 to $2.0 \mu\text{g m}^{-3}$ imply that future decreases in mean SO_4 -associated
37 OC concentrations would not exceed ~0.3 to $0.5 \mu\text{g m}^{-3}$. Seasonal OC concentrations,
38 largely identified with ozone (O_3), vary from 0.3 to $1.4 \mu\text{g m}^{-3}$ (~20% of the total OC
39 concentrations).

40

41 **1 Introduction**

42 In much of North America, organic aerosol (OA) represents approximately half of
43 average $\text{PM}_{2.5}$ mass concentrations in ambient air (Kanakidou et al., 2005). OA derives
44 from primary source emissions and secondary atmospheric processes involving reactions
45 of volatile organic compounds (VOCs) of anthropogenic and natural origins (see
46 appendix). The latter is widely recognized in the southeastern U.S. with its potential
47 source of VOCs from dense vegetation (Hand et al., 2012). Initial speculation about
48 secondary organic aerosol (SOA) in the Southeast from natural terpenoid compounds
49 dates back to 1991 (e.g., Pandis et al., 1991). With re-evaluation of particle yields from
50 isoprene acidic-photochemical oxidation in smog chambers, interest in natural SOA
51 focused on this species (e.g., Kroll et al., 2006). The early 2000s investigations involving
52 isoprene and terpenoids identified chemical mechanisms hypothetically applicable in the
53 ambient atmosphere as well as tracers for reaction products (e.g. Hallquist et al., 2009).
54 These hypotheses included accounting for the effect of acidity and photochemical
55 linkages with the gas and condensed phases; a part of this chemistry involves the
56 interactions with inorganic acids in the atmosphere—sulfur and nitrogen oxides, SO_2 and
57 NO_x . More recently, field studies have adopted measurements from aerosol mass
58 spectrometry combined with gas chromatograph and mass spectroscopy to track indicator

59 species for SOA components, including species associated with isoprene- sulfur oxide or
60 nitrogen oxide photochemistry (e.g., Gao et al., 2006; Surratt et al, 2007; Hatch et al.,
61 2011a,b; Budisulistiorini et al., 2013; Liao et al., 2015; Lin et al., 2013; 2014; Hu et al.,
62 2015; Kim et al., 2015; Xu et al., 2015a, b).

63 In parallel with advances in organic aerosol chemistry, workers explored different
64 indirect means of estimating SOA from VOC sources. In Atlanta, Lim and Turpin (2002)
65 used the carbon tracer method to calculate summertime SOA concentrations from
66 collected filter samples. In the Southeast, Zheng et al. (2002; 2006) used chemical tracers
67 extracted from filters to identify primary OA, noting that an incomplete mass balance
68 could be SOA. Kleindienst et al. (2007; 2010) and Lewandowski et al. (2013) used
69 chemical tracers to estimate SOA from isoprene and terpenes. The carbon tracer method
70 was expanded for natural species using carbon isotopes (e.g., Lewis et al., 2004; Tanner
71 et al., 2004; Zheng et al., 2006; Ding et al., 2008). The empirical approaches were
72 explored further by Yu et al. (2007) and Blanchard et al. (2008). Identification of water-
73 soluble carbon as an SOA indicator also has been used (e.g. Weber et al., 2007). The
74 various evolving methods have provided operationally defined OA as indicated
75 schematically in Figure S1.

76 The characterization of SOA in the Southeast is complicated by OA from open burning of
77 vegetation (e.g., Zhang et al., 2010; Hu et al., 2015). Like other combustion sources,
78 wildfires and prescribed burning appear to be important components of OA and SOA
79 (e.g., Zhang et al., 2010; Hidy et al., 2014; Washenfelder et al., 2015). OA composition
80 in the southeastern U.S. provides indications of emission source origins, but results have
81 not been consistent across studies (Table S1). SOA particularly is known to be a complex
82 description of emissions, followed by evaporation, condensation, and chemical
83 interactions during species aging in the atmosphere.

84 The ambiguities in accounting for OA sources and the chemistry of SOA helped motivate
85 a major suite of field experiments during the summer of 2013, the Southern Oxidant and
86 Aerosol Study (SOAS) (SOAS, 2014) and associated campaigns that comprised the
87 Southeast Atmosphere Study (SAS) (SAS, 2014). Ground-level measurements were
88 located at rural sites, with many studies situated at a Southeastern Aerosol Research and

89 Characterization (SEARCH) network monitoring location outside Brent, near Centreville,
90 Alabama (CTR) (e.g., Hu et al., 2015; Isaacman-VanWertz et al., 2015; Nguyen et al.,
91 2015; Washenfelder et al., 2015; Xu et al., 2015a; b), a site estimated to be regionally
92 representative (Hidy et al., 2014).

93 CTR and other SEARCH sites offer a long-term record of trace-gas and particle
94 observations (Hidy et al., 2014) that provide insight into the effects of anthropogenic
95 emission reductions on organic aerosol trends in the southeastern U.S. The SEARCH
96 record complements the six-week-long SAS and SOAS investigations of key atmospheric
97 processes and chemical reactions. Specific questions relevant to SOAS and SAS goals
98 that can be addressed using the SEARCH data include:

- 99 1. What fraction of measured organic carbon (OC) was emitted by combustion processes,
100 such as motor vehicle exhaust and biomass burning? How has this fraction responded
101 to emission reductions?
- 102 2. Over a long period of record, can the fractions of OA directly emitted in the condensed
103 phase (primary organic aerosol, POA) and of SOA formed in the atmosphere via
104 reactions of gaseous or condensed-phase precursors be quantified or constrained
105 based on diurnal, seasonal, and annual variations of OC, elemental (or black) carbon
106 (EC), ozone (O₃), sulfate (SO₄), and other aerometric measurements? How have
107 inferred SOA concentrations responded to emission reductions?
- 108 3. Do the long-term gas and particle measurements indicate how much biogenic SOA is
109 present on daily, seasonal, or annual time scales? How has SOA of biogenic origins
110 been affected by anthropogenic emission reductions?

111 This paper describes analyses of aerometric data from CTR and the other SEARCH sites
112 that address these questions. We apply five complementary data analysis methods that
113 provide insight into the sources of aerosol carbon in the Southeast relying on the long-
114 term SEARCH database. Because uncertainties and differences among previous studies
115 have been challenging to resolve due to inconsistent or ambiguous definitions and
116 terminology used to describe carbon measurements, an appendix defines terminology and
117 identifies unresolved questions. We adopt in part the concepts of aerosol evolution from

118 initial emission to multiscale ambient conditions postulated by Robinson et al. (2007),
119 noting accompanying uncertainties (e.g., Murphy and Pandis, 2010).

120

121 **2 Methods**

122 The data for this study of aerosol carbon derive primarily from long-term SEARCH
123 measurements obtained from up to eight operating sites, comprising four urban-rural or
124 urban-suburban pairs, between 1999 and 2013 (e.g., Hansen et al, 2003; Atmospheric
125 Research and Analysis [ARA], 2014; Hidy et al., 2014). The dataset includes particle
126 mass concentrations and composition, gases, and meteorological parameters (ARA, 2014)
127 as previously described in Hansen et al. (2003) and Edgerton et al. (2005; 2006). Special
128 data from ancillary experiments in the SEARCH network supplement the long-term data.
129 We also use emission data derived from the EPA National Emission Inventory (NEI),
130 augmented as described in Blanchard et al. (2013) and Hidy et al. (2014).

131 Multiple empirical methods are employed to understand OA sources and SOA formation
132 in the southeastern U.S., utilizing the SEARCH data to obtain a multi-year and multi-
133 season interpretation. The methods are: (1) comparison of observations with augmented
134 NEI emission estimates (Hidy et al., 2014) and receptor model predictions based on the
135 NEI, (2) comparison and correlation of measured OC with EC concentrations and use of
136 the OC/EC ratios as indicators of combustion-related emissions and SOA formation, (3)
137 computation of organic mass (OM)/OC ratios utilizing $PM_{2.5}$ mass and sums of species
138 concentrations as evidence for the presence of oxidized OA, (4) estimation of biomass
139 burning contributions to measured EC and OC using biomass burning tracers, and (5)
140 application of receptor modeling (principal component analysis, PCA, supplemented with
141 comparisons to positive matrix factorization, PMF) to identify and quantify atmospheric
142 processes affecting OA concentrations. Computational details are described within the
143 results and discussion section and in the supplemental information.

144

145 **3 Results and Discussion**

146 **3.1 Emission sources and the relation of ambient to emission trends**

147 This section incorporates previously published analyses by reference, extends them
148 through 2013, and integrates findings. Results related to emission changes are compared
149 with those obtained using other approaches in Section 3.6 (Synthesis).

150 Southeastern emissions in 2013 are shown by source category in Table S2; comparison
151 with 2008 emissions reported in Blanchard et al. (2013) indicates reductions since 2008.
152 Statistically significant ($p < 0.001$) relationships were found between mean annual $PM_{2.5}$
153 EC and OC concentrations at SEARCH sites and $PM_{2.5}$ EC and OC emissions between
154 1999 and 2013 (Hidy et al., 2014). Ambient EC trends were significantly related to both
155 mobile source and total EC emissions, whereas ambient OC trends were significantly
156 related to mobile source OC emissions but not to total OC emissions (Hidy et al., 2014).
157 $PM_{2.5}$ EC emissions in the southeastern U.S. declined by approximately half between
158 1996 and 2013 due to reductions of on-road and non-road motor vehicle emissions (Hidy
159 et al., 2014). Corresponding declines occurred in on-road and non-road motor vehicle
160 $PM_{2.5}$ OC emissions, but total $PM_{2.5}$ OC emissions showed little trend due to the
161 dominance of relatively constant biomass burning emissions (Hidy et al., 2014). Mobile
162 source OC emissions represent less than 10% of OC emissions in the Southeast
163 (Blanchard et al., 2013; Hidy et al., 2014) and only 4% as of 2013 (Table S2), with
164 biomass burning accounting for ~75% of OC emissions in emission inventories.

165 Using a receptor modeling approach, Blanchard et al. (2013) showed that $PM_{2.5}$ EC
166 emissions generally account for reported mean annual EC concentrations and trends in
167 the SEARCH network (Figure S2). Although the receptor model overpredicted EC
168 concentrations at the Jefferson Street (JST) site in Atlanta, Georgia, and underpredicted
169 EC concentrations at other sites, the EC trends predicted by the model from the inventory
170 agreed with observed EC trends. Larger observed ambient EC decreases at SEARCH
171 sites coincided with an EC emission decline occurring between 2005 and 2013 that
172 resulted from new Environmental Protection Agency (EPA) standards for diesel engines
173 and fuels (effective in 2007 for on-road vehicles, in mid-2010 for non-road mobile

174 sources, and in mid-2012 for rail and marine sources) (Hidy et al., 2014). Mobile sources
175 account for over 50% of EC emissions in the Southeast prior to 2007 (Blanchard et al.,
176 2013) and decline to ~40% by 2013 (Table S2), so ambient EC concentrations are
177 expected to decrease with declining mobile source EC emissions.

178 Contrasting with results for EC (as well as CO, NO_x, and SO_x), greater differences
179 between receptor model-predicted OC and measured OC trends were observed (Figure
180 S3). These differences occurred even when comparing model predictions to the fraction
181 of measured OC that was not associated with O₃ and SO₄ (inventory OC emissions do not
182 represent SOA deriving from biogenic emissions of isoprene and other gases). Ambient
183 OC trends were more pronounced than trends predicted by the model from the inventory
184 (Figure S3). However, the receptor model reproduces observed OC trends more readily
185 for sites where the mobile source contribution is greatest (Figure S3). Receptor-modeling
186 studies have consistently identified mobile source contributions to ambient PM_{2.5} mass
187 concentrations in Atlanta and Birmingham (e.g., Zheng et al., 2002; 2006; Baumann et
188 al., 2008; Lee et al., 2009); a recent analysis indicated that mobile sources contributed 0.8
189 to 2.8 μg m⁻³ to 2006 – 2010 PM_{2.5} mass concentrations (between 6 – 7% and 19 – 21%
190 of PM_{2.5} mass) in Atlanta and Birmingham (Watson et al., 2015). Measured ambient
191 concentrations of non-polar PM_{2.5} OC species associated with motor vehicles, such as
192 hopanes and steranes, declined substantially (>50 %) at BHM and JST between 2006 and
193 2010, linking mobile source emission reductions during those years with observed
194 decreases in urban OC concentrations (Blanchard et al., 2014a). As noted in the
195 appendix, emitted OC is not conservative, but is affected by evaporation and possibly
196 recondensation as secondary species, or by augmentation by SOA derived from gas-phase
197 emissions. A possible explanation for the observed OC trends is that diesel SOA
198 concentrations (which were not incorporated in the receptor model predictions) were
199 greater prior to adoption of new diesel emission regulations beginning in 2007. In
200 addition, changes in gasoline-engine SOA concentrations may have occurred. Reductions
201 of SO₂ emissions are also thought to have changed SO₄-associated SOA concentrations
202 over time (Xu et al., 2015a, b), but the chemical mass balance (CMB) model is set up to
203 predict OC that is not associated with O₃ and SO₄ (Blanchard et al., 2013).

204 Trends in mobile source VOC emissions paralleled trends in mobile source PM_{2.5} OC and
205 EC emissions (Hidy et al., 2014; Blanchard et al., 2013). Similar to OC emissions, mobile
206 source VOC emissions in the southeastern U.S. declined by approximately half between
207 1996 and 2013 due to reductions of on-road and non-road motor vehicle emissions (Hidy
208 et al., 2014), but total VOC emissions showed little trend due to dominance by relatively
209 constant VOC emissions from vegetation and soils (Table S2).

210 In summary, emission trends partially explain observed ambient EC and OC trends. For
211 OC, the link between inventory emissions and ambient concentrations is less definitive
212 than is the case for links between reductions of EC, CO, NO_x, and SO₂ emissions and
213 observed trends in ambient EC, CO, NO_y, SO₂, and PM_{2.5} SO₄ concentrations (Hidy et al.,
214 2014).

215 **3.2 Ambient EC and OC concentrations and trends**

216 Trends and spatial variations are evident for mean annual and seasonal EC and OC
217 concentrations (Table 1 and Figure 1). Mean EC concentrations were 2.0 to 3.5 times
218 greater at JST than at CTR, thereby indicating two- to three-fold greater influence of
219 combustion sources within Atlanta compared to rural CTR because EC is a tracer of
220 combustion (appendix). Mean OC concentrations were 1.0 to 1.8 times greater at JST
221 than at CTR, indicating urban sources of OC possibly superimposed on a relatively high
222 regional baseline. The ratio of JST EC to CTR EC declined from 2.8:1 to 2.1:1 between
223 the first and third five-year periods, while the JST OC to CTR OC ratio decreased from
224 1.5:1 to 1.2:1 between the first and third five-year periods. Since the ratio of JST
225 EC/CTR EC declined by 25% and the ratio of JST OC/CTR OC declined by 20%, the
226 decreases are comparable but the difference is consistent with a greater mobile source
227 influence at JST than at CTR. Both EC and OC concentrations exhibit decreasing trends
228 at all SEARCH sites (Hidy et al., 2014), particularly after 2007 but with a possible rise
229 between 2009 and 2011 (Figure 1). Higher mean monthly concentrations in 2011 were
230 followed by further decline in 2012 and 2013 (Figure 1). Whereas long-term ambient EC
231 and OC trends are predicted by EC and OC mobile source emission reductions (Section
232 3.1), changes between 2008 and 2013 are predicted from the emission inventory for EC
233 (Figure S2) but not for OC (Figure S3).

234 No season consistently exhibits the highest mean EC and OC concentrations but the CTR
235 mean OC concentrations and OC/EC ratios are highest during summer, interpreted as the
236 influence of aging and SOA formation during warmer months. In contrast, JST mean OC
237 and EC concentrations tend to be higher during autumn and winter (Table 1). In 2013, the
238 ratios of OC to total carbon (TC = EC + OC) in daily-average filter samples were greatest
239 at CTR during the SOAS campaign (Figure S4). This result suggests that rates of SOA
240 formation at CTR during SOAS exceed SOA formation rates at other sites in the region
241 and at other times of the year. The differences between JST and CTR mean summer OC
242 concentrations decline from $1.1 \mu\text{g m}^{-3}$ in 1999-2003 to less than $0.1 \mu\text{g m}^{-3}$ in 2009-
243 2013, interpreted as reductions of urban OC concentrations toward a regional baseline
244 level (Table 1).

245 Mean OC/EC ratios are higher at CTR than at JST, again consistent with regional-scale
246 aging of ambient aerosol and a relatively greater influence of SOA at CTR. The period
247 mean OC/EC ratios at JST range from 2.3:1 to 4.0:1, suggesting variable contributions
248 from multiple sources. For comparison, typical OC/EC ratios are ~ 1 in freshly emitted
249 motor vehicle emissions (Chow et al., 2004), with important differences among vehicle
250 types (McDonald et al., 2015), $\sim 5:1 - 20:1$ in near-source biomass burning plumes
251 (Andreae et al., 1996; Andreae and Merlet, 2001; Hobbs et al., 1996; Lee et al., 2005),
252 and potentially much greater than unity as oxidation and SOA formation proceed
253 (Robinson et al., 2007).

254 Temporal trends in ambient EC and OC correlated within individual sites and across the
255 SEARCH domain (e.g., CTR and JST, Figure 1), indicating regional coherence of trends
256 and seasonal variations for both EC and OC. The strong correlation of EC and OC at all
257 SEARCH sites, averaging times (annual, seasonal, monthly, daily), and seasons (Table
258 S3; Figure S5) indicates that combustion processes are a major source of OC. However,
259 significant correlations of SO_4 with both EC and OC during summer suggest the
260 influence of SO_4 on SOA formation in summer, consistent with results from SOAS (Xu
261 et al., 2015a, b; Budisulistiorini et al., 2015). OC correlates with both EC and SO_4 , but
262 for different reasons. Consequently, EC and SO_4 also correlate, but not as strongly and
263 not as consistently across time scales. In summary, the EC and OC measurements

264 indicate influence of multiple emission sources or atmospheric processes affecting all
265 SEARCH sites, though differently at urban and rural locations.

266 **3.3 OM/OC ratios**

267 More oxygenated OA has higher ratios of OM/OC, so OM/OC potentially serves as an
268 indicator of atmospheric aging (Turpin and Lim, 2001). A low value (e.g., OM/OC ~ 1.4
269 to 1.6) suggests little aging (i.e., POA is a large fraction of OA), whereas a high value
270 (e.g., > 2) suggests more aging (SOA is a large fraction of OA). For comparison, OM/OC
271 ratios are 1.2 for pentane (and higher molecular weight alkanes), 1.1 for isoprene, and 2.0
272 for isoprene epoxydiol (IEPOX) (a gas-phase intermediate of isoprene oxidation, yielding
273 SOA). The average motor vehicle OM/OC ratio is ~1.2 to 1.4 (Landis et al., 2007) while
274 biomass burning OM/OC averages ~1.4 to 1.8 (Reid et al., 2005).

275 We estimate the OM/OC ratio for the urban and rural SEARCH sites using a mass
276 balance computation based on particle composition. The sum of species concentrations,
277 including estimated particle-bound water (PBW) at laboratory temperature and relative
278 humidity (RH), is:

$$279 \text{ Sum of species} = f_1 \cdot \text{SO}_4 + f_2 \cdot \text{NO}_3 + f_3 \cdot \text{NH}_4 + \text{EC} + \text{OC} + \text{MMO} + \text{Na} + \text{Cl} \quad (1)$$

280 (inorganic species concentrations are from ion measurements). PBW at laboratory RH of
281 < 38% is represented by the coefficients f_1 (1.28), f_2 (1.15), and f_3 (1.25) (Tombach, 2004,
282 as derived from Tang et al., 1996). The coefficient f_1 is an average of the coefficients for
283 NH_4HSO_4 (1.27) and $(\text{NH}_4)_2\text{SO}_4$ (1.29), f_2 is the coefficient for NH_4NO_3 , and f_3 is a
284 weighted average reflecting higher SO_4 than NO_3 concentrations. MMO is the sum of the
285 concentrations of six crustal elements (Al, Ca, Fe, Mg, Si, Ti) (x-ray fluorescence [XRF]
286 spectroscopy measurements), expressed as oxides (Hansen et al., 2003). This estimate of
287 crustal mass is likely conservative, since it does not include Mn and the assumed Ca mass
288 (as CaO) would be less than the mass of CaCO_3 (if present). The carbon components,
289 metals, and chloride are not adjusted for retained water at laboratory temperature and
290 humidity. This creates a potential for uncertainty in the calculation, especially in the case
291 of OC. Atmospheric OC is known to be hygroscopic at elevated humidity, but
292 experimental data suggest that water retention is minimal at < 38% RH for laboratory

293 filter analysis (e.g., Malm et al., 2005; Taylor et al., 2011). Measurements made during
294 SOAS indicate that organic-associated water was less than ~25% of total particle water in
295 mid-day ambient samples when ambient RH was less than ~50% (Guo et al., 2015). We
296 estimate an OC PBW uncertainty in Eq. (1) by assuming that OC PBW is 10% of OC (f_{oc}
297 = 1.1), which would increase the calculated sum of species by 3% and decrease the
298 OM/OC (calculated below) by 0.1 units on average.

299 The difference between $PM_{2.5}$ mass and the sum of species concentrations is denoted as
300 “non-measured” (NM) mass:

$$301 \quad NM \text{ mass} = PM_{2.5} \text{ mass} - \text{Sum of species} \quad (2)$$

302 An upper bound for OM is calculated as $OM^* = OC + NM \text{ mass}$, which assumes that all
303 NM mass is associated with OA. Any mass that is missing from the computed sum of
304 species would bias NM mass high, thereby also causing OM^* to be higher than the true
305 OM. Similarly, underestimation of PBW would bias NM mass and OM^* high. We
306 estimate the combined effect of missing species and PBW to result in possible
307 overestimation of OM^*/OC by up to 0.2 units on average. An opposing bias potentially
308 arises in Equation 2, because the FRM sampler that is used by SEARCH to provide the
309 $PM_{2.5}$ mass measurement is known to lose volatile species (e.g., inorganic particle NO_3).
310 We recalculated Equation 1 by replacing the measured NO_3 and Cl concentrations (which
311 are the sum of a Teflon front filter and a nylon back-up filter located in the SEARCH
312 PCM sampler) with the Teflon filter concentrations. The effect was to reduce the
313 calculated sum of species, which then increased the calculated OM^*/OC by 0.2 units on
314 average. Therefore, we estimate the uncertainty in the calculated OM^*/OC ratios as ± 0.2
315 units. If no PBW is associated with inorganic species (SO_4 , NO_3 , NH_4), Equation 1 would
316 underestimate OM^*/OC by 0.5 units on average. However, inorganic PBW is expected
317 even at $RH < 38\%$, so this potential bias appears less plausible than the documented bias
318 in FRM $PM_{2.5}$ mass concentrations.

319 At all SEARCH sites, NM mass concentrations averaged 1.5 to 1.9 $\mu g m^{-3}$ (interquartile
320 range ~0.5 to ~2.5 $\mu g m^{-3}$ at all except YRK) during the most recent five-year period
321 (2009 to 2013; Na and Cl ions were not measured prior to 2008) (Figure S6). Daily NM
322 mass correlated with daily OC to varying degrees: r^2 was 0.2 – 0.3 at Birmingham,

323 Alabama (BHM), Gulfport, Mississippi (GFP), (rural) Oak Grove, Mississippi (OAK),
324 and 0.4 – 0.5 at CTR, JST, (rural) Yorkville, Georgia (YRK), (suburban) Outlying
325 Landing Field, Pensacola, Florida (OLF), and Pensacola, Florida (PNS). The average
326 OM^*/OC varied by site from 1.5 (BHM) to 2.0 (YRK) (Figure 2) ($\Delta OM^*/\Delta OC$
327 regression slopes of 1.6 to 1.9 without intercept terms, Figure S7), which suggests a
328 regionally characteristic but spatially and temporally variable mix of less-oxidized and
329 more-oxidized OA. The consistency of the mean values in the range of 1.5 to 2.0 (± 0.2)
330 indicates that relatively fresh emissions contribute a major portion of OA at both urban
331 and rural sites with variations in the degree of oxidation or SOA mass. However, higher
332 OM^*/OC and OM^*/EC occur in the warmest months (Figure 2), consistent with seasonal
333 SOA formation and the seasonal variations discussed above. Our mean OM^*/OC is lower
334 than reported in SOAS research – for example, mean CTR OM/OC of 2.16 from aerosol
335 mass spectroscopy [AMS] measurements (Xu et al., 2015a). For identical sampling
336 periods, our spring 2012 mean OM^*/OC was 1.34 at JST and 1.80 at YRK, which is
337 lower than mean OM/OC of 1.93 at JST and 1.98 at YRK reported by Xu et al. (2015b).
338 Our winter 2012-13 mean OM^*/OC was 1.51 at JST and 1.56 at YRK, which is higher
339 than mean OM/OC of 1.40 at JST and 1.31 at YRK reported by Xu et al. (2015b).
340 Comparisons are discussed further in Section 3.5.3.

341 **3.4 Biomass burning**

342 Emission inventories indicate that biomass burning, including prescribed burns, wildfires,
343 agricultural burns, and domestic heating, is the largest source of $PM_{2.5}$ OC emissions in
344 the Southeast on an annual-average basis (Hidy et al., 2014). Prescribed burns are the
345 largest source of biomass burning OC emissions, again on an annual basis (Hidy et al.,
346 2014). In the Southeast, prescribed burns are employed to manage roughly 4 million
347 hectares (ha) (~10 million acres) of land every year, primarily between January and
348 April; wildfires may occur year-round but are more frequent in warmer months (Wade et
349 al. 2000; Haines et al. 2001). Nearby (e.g., ~ 10 km) biomass burning plumes are
350 sometimes evident in CTR hourly data and substantially affect observed concentrations
351 of EC, OA, CO, NO_y , NH_3 , and O_3 (Figure S8). However, the cumulative effect of
352 widespread and potentially wide-ranging biomass burning on long-term ambient OA

353 concentrations is more difficult to determine. The available data record does not include
354 organic biomass burning tracers, such as levoglucosan, except during special studies such
355 as the six-week SOAS campaign. Alternatively, non-soil potassium (K) has been used as
356 an indicator of biomass combustion in previous studies (Calloway et al., 1989; Lewis et
357 al., 1988; Lewis, 1996; Pachon et al., 2010; 2013) and can be determined from K
358 measurements reported in the long-term SEARCH data. Using a single tracer species to
359 identify and quantify biomass burning contributions to ambient OA is subject to
360 important uncertainties, and potassium is an imperfect tracer of biomass burning. Zhang
361 et al. (2010), for example, showed that water-soluble K and levoglucosan correlate in
362 winter (when more biomass burning occurs in the southeastern U.S.) but not in summer.
363 However, levoglucosan and its associated AMS markers may persist in the atmosphere
364 for less than a day (May et al., 2012; Bougiatioti et al., 2014). Instability of organic
365 marker species could lead to differences in AMS biomass burning OA compared with
366 estimates made using K as a tracer.

367 Non-soil K (nsK) is estimated from coarse PM (PM_{coarse} or PM_{crs} , PM between 2.5 and 10
368 μm) and $PM_{2.5}$ XRF measurements of K and Si following the K tracer approach of
369 Pachon et al. (2013). Briefly, the method regresses measured K against species X
370 concentrations: $K = \alpha + \beta * X$ (where X derives primarily from crustal material). Si
371 measurements are used to represent the crustal species, X, because Si concentrations are
372 routinely well above the limits of detection and the correlations of Si with Al and other
373 known crustal elements indicate few or no interfering sources of Si. The correlations of
374 PM_{coarse} XRF K and Si are very strong, with consistent values of the slope $\beta = \Delta K / \Delta Si$ of
375 0.10 to 0.13 and $r^2 \sim 0.8$ at all sites (Figures S9 – S11). These slopes therefore define the
376 expected ratio of K/Si in crustal material in the region. The ratios are lower than, but
377 consistent with, a value of 0.15 ± 0.01 reported for data from Phoenix, AZ (Lewis et al.,
378 2003). In contrast to PM_{crs} , $PM_{2.5}$ measurements exhibit large excesses of K over the
379 expected K/Si ratios, indicating the presence of one or more non-crustal sources of $PM_{2.5}$
380 K (Figures S9 to S11). For each plot, fine-particle K vs. Si forms one “branch” that falls
381 on the line defined by coarse-particle K vs. Si, indicating similar relationships between K
382 and Si within fine and coarse fractions of crustal PM. High fine-particle K concentrations

383 also occur at lower-than-average fine Si concentrations. We apply the slopes β to
384 compute $nsK = K - \beta * Si$ from $PM_{2.5}$ data (Figure S9). The agreement between computed
385 nsK and measured water-soluble K (K ion, KI; measured beginning 2008) supports the
386 interpretation of non-soil K as an indicator of biomass burning K (Kbb) (which is water-
387 soluble) at rural inland sites such as CTR (Figure S9). Although computed Kbb exceeds
388 measured K ion concentrations by $\sim 0.02 - 0.03 \mu g m^{-3}$ on average, the difference may
389 relate to the differing resolutions and sensitivities of the XRF and ion measurements
390 (Figure S9). Later analyses (Section 3.5.2) link CTR Kbb with species (including CO and
391 EC) deriving from combustion. Possibly, both K ion and computed nsK could also have a
392 marine origin at some coastal sites (e.g., OLF) or an industrial process origin at some
393 urban sites (e.g., BHM). Detailed review of computed nsK indicated that all $nsK > 0.4 \mu g$
394 m^{-3} occurred on or one day after the 4th of July and January 1 US holidays, and only at
395 urban sites (Figure S11). This result appears to indicate fireworks as a source of nsK on
396 such occasions. Other than samples from January 1 and 2 and from July 4 and 5, we
397 identify nsK as biomass burning K (Kbb), recognizing some uncertainty in this
398 identification for BHM and coastal sites. Since nsK can be computed from the XRF
399 measurements of K and Si for the full SEARCH record (1999 to 2013), whereas K ion
400 measurements commenced in 2008, we use nsK as our biomass burning tracer. After
401 exclusion of obvious high-K events (holiday fireworks), our identification of nsK as an
402 indicator of biomass burning (Kbb) could introduce a bias toward overestimation in the
403 calculation of OCbb, discussed below, if other sources of water-soluble K are important.
404 The ratio of TC to Kbb (TCbb/Kbb) in biomass burning is known to vary widely among
405 fire types (e.g., wildfires differ from prescribed burns) and among fire stages (e.g.,
406 temperature, or flaming vs. smoldering). The variability of emissions among and within
407 fires implies that biomass burning tracers are more useful for estimating average impacts
408 than for quantifying burn contributions during individual events. We use a single average
409 scaling factor based on consideration of emissions information (Hidy et al., 2014), which
410 we check using the correlation of modern C with non-soil K (Figure S12). Inventory
411 annual average TCbb/Kbb for fires is in the range 28:1 – 36:1 (Blanchard et al., 2013).
412 For fires (prescribed burns, wildfire, agricultural field burns) plus area sources (largely

413 open burning from agricultural, construction, and yard waste), the 2013 ratio of
414 TC_{bb}/K_{bb} is ~ 23:1 (Table S2). The ratio varies among emission source profiles from
415 lower values of 5:1 and 7:1 (solid waste combustion and agricultural burning,
416 respectively) to an intermediate value of 19:1 (wildfire) and higher values of 43.5:1 (slash
417 burning) and 61:1 (residential wood combustion) (EPA, 2015; Reff et al., 2009). Our
418 assumed fixed scaling factor of 32 for TC_{bb}/K_{bb} is similar to carbon isotope data from
419 CTR winter samples (Figure S12, CTR regression slope $\Delta TC_{\text{modern}}/\Delta K_{\text{bb}} = 43$), when
420 prescribed burns are more common and SOA formation rates are lower. The higher slope
421 of $\Delta TC_{\text{modern}}/\Delta K_{\text{bb}} = 71:1$ at JST could reflect a different type of biomass burning (e.g.,
422 residential wood combustion), while the lesser correlation of modern TC with non-soil K
423 (assumed to represent K_{bb}) at BHM and higher slope at PNS potentially reflect source
424 variability or the confounding influence of industrial (BHM) or marine (PNS) sources of
425 non-soil K. The mean ratio of wood-burning OC concentrations determined by
426 Kleindienst et al. (2010) using organic tracers (20 samples, collected in May and August
427 2005, paired by site and date) to K_{bb} concentrations is 20:1 (varying by site from 16:1 at
428 BHM and CTR to 18:1 at PNS and 29:1 at JST). This result agrees with the inventory
429 TC_{bb}/K_{bb} of ~ 23:1 averaged across fires and area sources (Table S2) assuming that the
430 corresponding ratio of wood-burning TC/K_{bb} is ~10% higher than wood-burning
431 OC/K_{bb}. Since prescribed burns and residential wood combustion (higher TC_{bb}/K_{bb})
432 generally occur during winter months, whereas wildfires, agricultural field burns, and
433 waste burning (lower TC_{bb}/K_{bb}) may occur during warmer months, our assumed fixed
434 scaling factor of 32:1 for TC_{bb}/K_{bb} likely fails to capture some of the seasonal
435 variability in TC_{bb}. A higher scaling ratio (e.g., $\Delta TC_{\text{bb}}/\Delta K_{\text{bb}} = 32$ rather than 20) would
436 yield higher computed TC_{bb} and therefore higher OC_{bb}. Based on $\Delta OC/\Delta EC$ in actual
437 biomass burning events observed at SEARCH sites (Figure S8), we compute OC_{bb} =
438 0.9*TC_{bb} (the ratio OC_{bb}/TC_{bb} could be higher in some burn events). Considering the
439 range among SEARCH sites of winter $\Delta TC_{\text{modern}}/\Delta K_{\text{bb}}$ (22:1 to 82:1, Figure S12), the
440 variability of TC_{bb}/K_{bb} among source types, and the possibility that K_{bb} could be
441 overestimated if there are sources other than biomass burning that contribute to nsK, we
442 estimate the uncertainty range for OC_{bb} as -50% to +100% (factor of two) subject to the
443 constraint that OC_{bb} < OC.

444 CTR monthly-average concentrations indicate a downward trend in OC but not in
445 computed OC_{bb}, so that OC_{bb} has become a larger fraction of OC at CTR since 2007
446 (Figure 3). The absence of trend in computed OC_{bb} reflects the absence of trend in
447 measured K and computed nsK. OC_{bb} tends to be higher in winter months, when
448 prescribed burns are more common and residential heating needs are greatest, but OC_{bb}
449 is present during all seasons (Figure 3) and at all SEARCH sites (Figure S13). Retene, a
450 tracer of coniferous wood combustion, is evident at the sites where it was measured
451 (urban BHM and JST) with a pronounced seasonal cycle (Figure S14). This seasonality
452 could indicate that the summer OC_{bb} has been overestimated, or it could indicate that
453 retene loss rates are greater during warmer months. Retene emissions from prescribed
454 burning in the Southeast are highly variable and depend largely on the amount of
455 softwood present in the fuel. Since historical fire suppression has led to the accumulation
456 of significant amounts of hardwood in a thick midstory of pine-dominated forests (e.g.
457 Provencher et al., 2001, Varner et al., 2005), retene is not considered a unique indicator
458 for prescribed burning emissions in the Southeast.

459 The analysis of K measurements from the SEARCH data reinforces the conclusion that
460 biomass burning is an important component of combustion-related OA in the SEARCH
461 domain, at all sites and in all seasons. The contribution is especially important for
462 regional-scale OA, as suggested by the CTR data. Uncertainties in the estimation
463 procedure and scaling factors imply that our computed CTR mean OC_{bb} ($1.6 \mu\text{g m}^{-3}$,
464 1999 – 2013 average) could be up to twice as high as the true mean OC_{bb} concentration.
465 If so, actual mean 1999 – 2013 OC_{bb} would be $0.8 \mu\text{g m}^{-3}$, which is higher than AMS
466 mean biomass burning OA (10%, or $\sim 0.25 \mu\text{g m}^{-3}$ OC) at CTR during the six-week
467 SOAS period (Xu et al., 2015a, b). Although the majority of brown carbon aerosol mass
468 during SOAS is attributed to biomass burning rather than to SOA, biomass burning did
469 not contribute the majority of OA (Washenfeller et al., 2015). As previously noted, more
470 biomass burning occurs in the southeastern U.S. during cooler months than during mid-
471 summer (Zhang et al., 2010), so the SOAS campaign is expected to show less biomass
472 burning than during other months. Reported AMS mean biomass burning OA
473 concentrations were higher at JST ($\sim 0.5 \mu\text{g m}^{-3}$ OC during May and December 2012) and
474 at YRK ($\sim 0.6 \mu\text{g m}^{-3}$ OC during December 2012 and January 2013) (Xu et al., 2015a, b).

475 Due to the loss of organic tracers on a time scale of about a day or less, the biomass
476 burning OA that is estimated using AMS is thought to yield an estimate of relatively
477 fresh burning as compared to aged regional burning levels (Xu et al., 2015a, b). Estimates
478 of a regional pool of more aged biomass burning OA are not available. If the reported
479 AMS biomass burning OA concentrations are, e.g., ~50% lower than the sum of fresh
480 and aged biomass burning OA, the resulting sum ($1 \mu\text{g m}^{-3}$ OC) would fall within our
481 OCbb uncertainty range. The lack of long-term trend in OCbb (Figure 3) occurs
482 regardless of scaling uncertainties (assuming constant scaling of OCbb to Kbb), because
483 no trend exists in either K or Kbb concentrations.

484 **3.5 Principal component analysis**

485 Important insight into the origins of ambient aerosol can be obtained with multivariate
486 statistical methods, such as principal component analysis (PCA), which is a well-
487 established method for PM source apportionment (Dattner and Hopke, 1982). PCA
488 generates mathematically independent groupings of measurements based on the
489 correlations among the measured variables (classically, the groups are geometrically
490 orthogonal to one another). The number of groups reproduces as large a fraction of the
491 total variance of a data set as possible subject to optimization criteria, typically
492 explaining ~75 to 80% of the variance of, e.g., ~20 to 25 air pollutant species
493 concentrations with ~5 to 10 groups, also known as factors or components. Although
494 PCA factors may be identifiable with emission sources in some applications, factors
495 fundamentally represent correlations among species and potentially reflect a variety of
496 aerometric processes (e.g., secondary species formation, meteorological effects). In our
497 application, we interpret PCA factors as associations among species that are indicative of
498 variations in the chemical environment, and refer to such species associations as
499 components for brevity. A related methodology, positive matrix factorization (PMF)
500 (U.S. EPA, 2014), differs in part from PCA in that PMF constrains factors to positive
501 values. This constraint is physically realistic if PCA factors are interpreted as unique
502 emission source contributions. The negative values permitted by PCA are in fact
503 meaningful and informative if, in addition to emissions, factors represent a larger suite of

504 physical and chemical processes (e.g., deposition; chemical loss processes; contrasts
505 between inland versus marine air mass transport) as well as species origins.

506 **3.5.1 Application**

507 We report two main versions of PCA, with additional versions used for sensitivity tests
508 and auxiliary information. *PCA1* is applied to measurements made at SEARCH sites
509 from 2008 through 2013. The 23 gas and PM_{2.5} measurements comprise daily-average
510 concentrations of PM_{2.5} EC and OC (thermal-optical reflectance, TOR), daily averages of
511 gases NH₃ (measured continuously or at 24-hour resolution) and continuous NO_x and
512 NO_z, secondary species (daily peak 8-hour O₃, plus PM_{2.5} SO₄, NH₄, and NO₃), and PM_{2.5}
513 crustal elements (XRF measurements of Al, Si, and Fe), species associated with salts
514 (PM_{2.5} Na, Cl, Mg, and Ca ions), and trace metals (PM_{2.5} Zn, Cu). Both daily averages
515 and daily 1-hour-maxima of gases (CO and SO₂) are included to match the temporal
516 resolution of the other daily data while also potentially capturing shorter-duration plumes.
517 Water-soluble PM_{2.5} K (K ion) is included as a potential indicator of biomass
518 combustion. Because some species used in PCA1 were not measured throughout the 15-
519 year SEARCH program, *PCA2* is carried out to interpret long-term OC trends from 1999
520 through 2013. PCA2 excludes measurements that commenced in 2008 (water-soluble Ca,
521 Mg, K, Na, and Cl). XRF Ca and nsK are used instead of water-soluble Ca and K,
522 respectively. Without Na and Cl in PCA2, salt is not detectable, as will be discussed. NH₃
523 is excluded from PCA2, since those measurements began in 2004. Daily-average O₃ is
524 included in PCA2 to complement daily peak 8-hour O₃.

525 The sensitivity of our results to the choice of statistical method is examined by comparing
526 PCA1 and PCA2 and by using additional PCA and PMF applications. As described in
527 Section 3.5.3, the range of results obtained from PCA1, PCA2, other PCAs, and PMF is
528 used to estimate uncertainty. The additional PCA applications are carried out by using
529 special data, different suites of measurements, or different measurement periods. NMOC
530 measurements made every day at JST from 1999 through 2008 are incorporated to
531 generate *PCA3* as a modification of PCA2 (no ions and only XRF elements, and shorter
532 time period). Alternate versions of PCA2 are carried out for 2004 – 2013 CTR data to see
533 if factor loadings are robust and relatively insensitive to the choice of seasonal indicators

534 (*PCA4* and *PCA5*). The EPA PMF model (version 5; US EPA, 2014) was applied to the
535 same CTR and JST measurements used in *PCA2*. PMF requires estimates of
536 measurement uncertainty, which may be species-specific or even sample-specific. Two
537 sets of uncertainty estimates were employed: uniform (10% of species concentrations)
538 (*PMF1*), and species-specific (incorporating detection limits and species uncertainties of
539 5 to 25% of measured concentrations) (*PMF2*).

540 For PCA applications, the daily OC concentrations at each site are apportioned using
541 daily PCA factor scores. The OC apportionment is carried out by multiple regression of
542 daily OC concentrations against daily factor scores, retaining those that are statistically
543 significant ($p < 0.05$). Since the PCA components are orthogonal, the regression
544 coefficients are more stable than would be the case for multiple regression against
545 various tracer species, which are typically intercorrelated. The PMF model generates
546 source contributions internally.

547 **3.5.2 PCA Components**

548 *PCA1* and *PCA2* reveal consistent sets of species associations, resulting in 6 – 8 principal
549 components at each SEARCH site (Table 2). For clarity, we designate the components as:
550 (1) combustion, (2) crustal, (3) seasonal, (4) SO₂, (5) SO₄, (6) metals, (7) salt, and (8)
551 other. These names are used as descriptors, rather than as designated emission sources.
552 Component characteristics are discussed below. The full orthogonal solutions are shown
553 in the supplement (Tables S4 to S11). The values in Tables S4 to S11 are the coefficients
554 of the linear combinations of standardized species concentrations (daily concentration
555 less mean divided by standard deviation); each tabled value is also the correlation (r)
556 between a given species and a particular component. High (~ 1) or low (~ -1) values
557 indicate high correlation or anti-correlation, respectively; both are meaningful. A value
558 near zero indicates little or no correlation, so values in the range of ~ -0.5 to 0.5 represent
559 associations ranging from moderate anti-correlation (-0.5) to zero correlation to moderate
560 correlation (0.5).

561 The OC apportionments indicate statistically-significant relationships between OC and
562 four to seven PCA components (Tables S12 and S13). Mean contributions of each
563 statistically-significant component to daily OC at each site using both *PCA1* and *PCA2*

564 are summarized in Table 3; these contributions are expressed as percentages of total OC
565 in Table S14. PCA1 and PCA2 each indicate that OC is associated with multiple
566 components at all sites. Except at YRK and OLF (PCA2 only), the overall OC
567 associations are strongest for the combustion component (Tables S4 to S11).

568 The PMF source profiles varied depending on the choice of uncertainty inputs, but
569 yielded average OC apportionments that were qualitatively comparable to PCA2 (Figure
570 S15). The PMF crustal OC and SO₄-associated OC concentrations were comparable to
571 PCA (Figure S16). However, PMF source profiles combined CO and O₃, whereas PCA
572 tended to separate O₃ from CO, leading to differences in the apportionment of OC to
573 combustion and seasonal components (Figure S16). Differences between PCA and PMF
574 occur in part because the PCA seasonal component generally comprised contrasts (e.g.,
575 positive O₃, negative inorganic particulate NO₃) whereas PMF forced positive solutions.
576 In these applications, PCA predicted high OC concentrations more accurately than PMF
577 did (Figure S17).

578 Combustion. All sites exhibit a suite of species associated with combustion processes
579 (EC, OC, CO, K_{bb} or K ion, NO_x or NO_z). The variations in combustion associations
580 among sites suggest different source mixes, differences in air mass ages (e.g., fresh
581 emissions at urban sites, more aged emissions at rural sites), or differing transport of
582 polluted air masses. For example, NO_z is more strongly associated than NO_x with the
583 combustion component at the two most rural sites, CTR and OAK. OC associated with
584 the combustion factor could therefore comprise material that would be classified as either
585 POA or SOA by other analytical approaches (e.g., HOA or MO-OOA by AMS).

586 Mean combustion OC ranges from 0.7 to 1.6 μg m⁻³ for PCA1 (2008 – 2013) and from
587 1.5 to 2.6 μg m⁻³ for PCA2 (1999 – 2013), except at YRK (Table 3). Daily PCA1 and
588 PCA2 combustion OC concentrations are correlated at all sites (Figure S18). Mean
589 absolute differences between PCA1 and PCA2 computed combustion OC range from 0.1
590 to 0.7 μg m⁻³ (not tabled). However, the mean PCA1 and PCA2 combustion OC
591 concentrations are averaged over different time periods, so the differences in their
592 averages are partly due to declining EC, CO, and NO_x concentrations (Table 1). Trends in

593 OC components are discussed in Section 3.4.4. Mean PCA2 combustion OC ranged from
594 25 to 63% of mean OC concentrations (Table 3).

595 Various combustion processes are expected to influence individual SEARCH sites to
596 different degrees. CTR OC_{bb} correlates significantly ($p < 0.0001$) with PCA1 and PCA2
597 combustion-associated OC ($r^2 = 0.54$ and 0.58 , respectively, Figure S19a), suggesting
598 that the combustion component at CTR is primarily associated with biomass burning.
599 Whereas OC_{bb} is computed from K_{bb} (Section 3.4), PCA1 and PCA2 combustion OC
600 concentrations are determined from the principal component association of CO, EC, and
601 either K ion (PCA1) or K_{bb} (PCA2) (Table S5). The association of K ion and K_{bb} with
602 CO and EC at CTR links potassium with a combustion process. At BHM and JST,
603 multiple regression of combustion OC against NO, gas-phase organic species (Blanchard
604 et al., 2010), and non-polar OC compounds (including PAHs and iso/anteisoalkanes, or
605 hopanes and steranes) (Blanchard et al., 2014a) indicates an association of fresh
606 emissions (NO) and non-oxidized organic compounds with PCA combustion OC (Figure
607 S19b). The urban PCA combustion factor associates CO, EC, and daily-average NO_x; 1-
608 hour maximum NO and non-oxidized organic compound concentrations were not used in
609 determining either PCA1 or PCA2 (Tables S4 and S7). Urban PCA combustion OC is
610 more likely attributable primarily to motor vehicle exhaust emissions than to biomass
611 burning.

612 Crustal. A crustal component is present at all sites, associated with Al, Si, Fe, and, to
613 varying degrees, Ca. At BHM, Fe associates more prominently with a metals component,
614 consistent with previous studies indicating the impact of industrial facilities (including
615 metals fabrication) on PM_{2.5} at BHM (Baumann et al., 2008; Blanchard et al., 2014b).

616 The mean crustal-associated OC concentrations vary from 0.1 to 0.3 $\mu\text{g m}^{-3}$ at inland sites
617 (Table 3). Coastal sites exhibit non-significant, minor, or inverse associations of OC with
618 crustal elements (-0.1 to $0.1 \mu\text{g m}^{-3}$, Table 3). Inverse associations indicate that OC
619 concentrations at coastal sites are lower than average when Al, Si, and Fe concentrations
620 are elevated. PCA1 and PCA2 crustal OC concentrations correlate (Figure S20) and
621 crustal OC correlates with Si (Figure S21). Crustal-associated OC could derive from
622 region-wide phenomena (e.g., transport of Saharan dust), but may also stem from

623 ubiquitous and widely distributed activities that suspend crustal material. Potential
624 sources include soil-derived OC (e.g., agricultural activities, construction, or road dust),
625 or biomass burning that lofts crustal material (e.g., through plowing material into debris
626 piles). Road dust is known to include OC among its constituents (e.g., McDonald et al.,
627 2013). There are two episodes with high crustal OC at CTR during June 2013. Elevated
628 concentrations of Al, Si, and Fe co-occurred at all SEARCH sites during June 9 – 13 and
629 June 23 – 28, 2013, thus suggesting region-wide events. Back-trajectory calculations
630 indicate southerly air flow during these times. Trajectories arrived at CTR and JST after
631 ~24 hours overland transport from the Gulf coast, whereas trajectories arrived at OLF
632 from overwater transport. At other times, elevated concentrations of crustal elements
633 occur at single sites, indicating more local events.

634 Seasonal. A seasonal component is present at all sites, but in two forms: positive O₃ and
635 NH₃ (if measured), along with negative inorganic particulate NO₃, at BHM PCA2, CTR,
636 GFP, JST PCA1, OAK, OLF, PNS, and YRK, or with reverse signs (e.g., relatively weak
637 negative O₃) at BHM PCA1 and JST PCA2. As noted, sign reversals represent a change
638 in coordinate directions and need not have physical significance; however, the association
639 of OC with the seasonal component may differ depending on sign (discussed below). We
640 denote this component “seasonal” rather than “photochemical.” While this factor has
641 photochemical properties, it is comprised of species with seasonality variations that result
642 from multiple processes: emissions (NH₃), photochemistry (O₃), and temperature- and
643 RH-sensitive thermodynamic equilibrium (inorganic particulate NO₃). The seasonal
644 component evidently represents seasonal variations not otherwise described by the
645 seasonal variations of the crustal, SO₄, and “other” components. Because of the strong
646 connection of the seasonal component to O₃, seasonal OC is plausibly related to the LO-
647 OOA component reported by Xu et al., (2015a; b). LO-OOA exhibits a strong diurnal
648 pattern, with night maxima and day minima (Xu et al., 2015a; b). However, the LO-OOA
649 diurnal variation is opposite to O₃ diurnal variations, which exhibit daytime maxima.
650 Since PCA was applied to daily-resolution data, it is not possible to directly compare the
651 PCA seasonal OC to time-resolved LO-OOA. We note that meteorological conditions
652 that result in high peak daily O₃ concentrations (with higher seasonal OC concentrations)
653 are also conducive to nitrate radical formation, which exhibits night-time maxima and is

654 associated with LO-OOA (Xu et al., 2015a; b). Further comparisons are provided in
655 Section 3.5.3.

656 The mean PCA1 seasonal-component OC (OC associated with higher O₃, higher NH₃,
657 lower NO_x, or lower PM_{2.5} inorganic NO₃) ranges from 0.4 to 0.6 μg m⁻³ at all sites (e.g.,
658 23% of OC at CTR, 13% at BHM and JST, 28% at OLF), except at YRK where the
659 average is 1.0 μg m⁻³. The positive association with O₃ suggests that this OC component
660 represents SOA formation from either or both anthropogenic and biogenic precursors.
661 PCA2 seasonal OC correlates with PCA1 seasonal OC, except at JST. The JST PCA2
662 seasonal OC shows an inverse correlation (Figure S22), indicating that the seasonal
663 component represents higher winter (lower O₃, higher NO₃) OC concentrations, possibly
664 pointing to an influence from domestic wood combustion for heating. The positive
665 association of OC with O₃ is quantified within the JST PCA2 SO₄ component. The mean
666 absolute differences between PCA1 and PCA2 seasonal-component OC concentrations
667 range from 0.2 to 0.5 μg m⁻³.

668 Sulfate. SO₄ and NH₄ are always associated and usually represented by a single
669 component, denoted “SO₄.” However, SO₄ and NH₄ are part of the seasonal component
670 for PNS and YRK PCA2, suggesting that differentiation of the SO₄ and seasonal
671 components is subject to uncertainty. O₃ is associated with both seasonal and SO₄
672 components.

673 All SEARCH sites show an association of OC with SO₄ ranging from 0.3 to 0.6 μg m⁻³
674 on average for PCA1 and from 0.5 to 1.0 μg m⁻³ on average for PCA2 (Table 3), with
675 PCA2 SO₄ OC representing 15 to 44% of the 1999-to-2013 mean OC concentrations
676 (15% at BHM; 22 – 25% at CTR, GFP, JST, and OAK; 44% at OLF). Mean PCA1
677 associations of OC with SO₄ were 14% of OC at CTR, 15% at BHM, 18% at OLF, 10%
678 at JST, and 11% at YRK. PCA1 and PCA2 SO₄ OC concentrations are correlated (Figure
679 S23) with mean absolute differences in PCA1 and PCA2 SO₄-associated OC
680 concentrations of 0.2 to 0.5 μg m⁻³; PCA2 did not separate the seasonal and SO₄
681 components at PNS and YRK (Tables S10 and S11). The mass of OC associated with
682 SO₄ averages 20 to 30% of the SO₄ concentrations (Figure S24), so that SO₄-associated
683 OC concentrations decline over time along with decreasing SO₄ concentrations. The

684 presence and relative importance of SO₄-associated OC is consistent with research
685 indicating the role of SO₄ in transferring isoprene gas-phase reaction products to the
686 condensed phase (e.g., Surratt et al., 2007; Xu et al., 2015a; b). Seasonal variations,
687 discussed below, also support biogenic origins of SO₄-OC. The quantitative relationship
688 of our SO₄-associated OC factor to SO₄ is the same as the relationship between isoprene
689 OA and SO₄, which Xu et al. (2015a, b) reported as 0.42 μg m⁻³ isoprene OA per 1 μg m⁻³
690 SO₄. Based on their reported OM/OC for isoprene OA (1.97), their result is 0.21 μg m⁻³
691 isoprene OC per 1 μg m⁻³ SO₄. For CTR (2008 – 2013, n = 383 days), we obtain 0.216 (±
692 0.008, 1 SE) μg m⁻³ SO₄-associated OC per 1 μg m⁻³ SO₄ (PCA1), 0.190 (± 0.004, 1 SE)
693 μg m⁻³ SO₄-associated OC per 1 μg m⁻³ SO₄ (PCA2), 0.213 (± 0.003, 1 SE) μg m⁻³ SO₄-
694 associated OC per 1 μg m⁻³ SO₄ (PMF1), and 0.211 (± 0.001, 1 SE) μg m⁻³ SO₄-
695 associated OC per 1 μg m⁻³ SO₄ (PMF2).

696 SO₂. The SO₂ component, present at all sites, identifies influences of relatively fresh
697 plumes, whether from electric generating units (EGUs), industrial, or other SO₂ sources.
698 At CTR, NO_x is more strongly associated with the SO₂ component than with the
699 combustion component, consistent with relatively less aged plumes and more aged
700 general combustion influence. Differences between urban and rural sites are evident; for
701 example, OC at CTR and YRK is not significantly related to the SO₂ factors, but OC is
702 related to the SO₂ factors at urban sites. This difference indicates the influence of SO₂
703 emission sources within urban areas, consistent with visual observations and
704 measurements made near emission sources in Birmingham (Blanchard et al., 2014b).

705 OC associated with SO₂, indicative of fresh emissions, accounted for 0.07 to 0.37 μg m⁻³
706 on average (12% of OC at BHM, 2% at JST, 7% at GFP, 20% at OAK, and 10% at OLF,
707 none at other sites using PCA1) (Tables 3 and S14). PCA1 and PCA2 SO₂ OC
708 concentrations are correlated (Figure S25).

709 Salt. A salt (or saltlike) component (of marine or other origins) is evidenced by Na, Cl,
710 and Mg in PCA1. Na appears as a separate “other” component for JST PCA1, suggesting
711 multiple urban sources of one or more of these species, while JST PCA1 “salt” is defined
712 by K, Cl, and Mg. These species are not necessarily unique marine tracers; various
713 combustion processes generate Cl emissions, for example.

714 Coastal sites show an inverse association of OC with Na and Cl (sea salt) (Table S14) and
715 a negative mean OC contribution from salt (Table 3). We interpret this result as evidence
716 that OC concentrations are lower at coastal sites when marine salt species concentrations
717 are higher (i.e., anti-correlated), indicating that marine air masses are not an important
718 source of OC. In contrast, mean salt-associated OC ranges from 0.14 to 0.15 $\mu\text{g m}^{-3}$
719 (BHM and YRK) to 0.64 $\mu\text{g m}^{-3}$ (JST). The species associations for the BHM and JST
720 salt components suggest urban influences precluding identification of the salt component
721 with marine air masses. Because K is associated with the JST “salt” component (and not
722 with the JST combustion component) and Na is associated with the JST “other”
723 component, it is possible that JST “salt” OC represents biomass combustion while the
724 JST combustion component primarily represents motor vehicle exhaust.

725 Metals. Cu and Zn appear on a metals component at six sites (BHM, CTR, GFP [PCA2],
726 JST [PCA2], OAK, and OLF [PCA2]); otherwise, Cu and Zn are associated with
727 combustion or are split between the metals and “other” components. The Cu and Zn
728 correlations range from $r = 0.1$ to 0.3 in the full 1999 to 2013 data set, which does not
729 suggest a simple or strong association between these two species. At JST, Cu correlates
730 with Pb.

731 Other. A component designated as “other” is present for BHM PCA1, GFP PCA1, JST
732 PCA1, PNS PCA2, and YRK PCA1 and PCA2, indicating variability at urban and near-
733 urban (YRK) sites not otherwise represented by the major components (Table 2).

734 **3.5.3 Intercomparisons and uncertainty**

735 For PCA3 (Table S15), the sum of alkanes, sum of aromatics, and α -pinene are
736 associated with the combustion component, whereas isoprene is associated predominantly
737 with the SO_4 component. The measured alkane and aromatic species are known
738 constituents of motor vehicle exhaust (Blanchard et al., 2010), consistent with a mobile
739 source contribution to the JST combustion component. Correlations between α -pinene
740 and CO, EC, and NO_x range from $r = 0.5$ to 0.6 , mathematically associating these species,
741 but the physical processes underlying the correlation are ambiguous (e.g., seasonal or
742 meteorological versus common source emissions). Isoprene and pinenes can be factors in

743 O₃ formation, and the association of isoprene with SO₄ could arise from a common
744 seasonality or from atmospheric chemical processes generating SOA from isoprene
745 (Surratt et al., 2007; Xu et al., 2015a, b). Additional work is needed to more fully
746 interpret VOC species associations.

747 PCA4 and PCA5 yield consistent results when NH₃ or daily-average O₃ are either
748 included or excluded from the analysis (Table S16).

749 The ranges of mean OC concentrations associated with each PCA component as obtained
750 from the various applications are listed for CTR, JST, and YRK in Table 4. Uncertainties
751 in the mean OC concentrations associated with each PCA component are estimated as
752 one-half the ranges for CTR and JST (comprising both PCA and PMF applications) and
753 the full ranges for YRK (PCA applications only), which generally yield comparable
754 uncertainties.

755 A summary of our PCA1 results compared to the 2012 – 2013 source apportionments
756 reported by Xu et al. (2015a; b) is shown in Tables S17 through S19. For these
757 comparisons, we determined the PCA1 means by matching days to each of the Xu et al.
758 (2015a; b) multi-week study periods. The PCA1 combustion OC tends to compare in
759 magnitude to AMS hydrocarbon-like OA (HOA), biomass burning OA (BBOA), cooking
760 OA (COA) (when one or more such factors are found) or to more-oxidized OA (MO-
761 OOA). The last correspondence would be expected to the extent that MO-OOA includes
762 oxidized motor vehicle exhaust, other anthropogenic combustion emissions, or biomass
763 burning (Xu et al., 2015a, b). As previously noted for CTR, PCA SO₄-associated OC
764 concentrations and AMS isoprene OA concentrations exhibit nearly identical regression
765 relationships with SO₄ concentrations. Some differences between mean PCA SO₄-
766 associated OC and mean AMS isoprene OA (converted to OC) percentage
767 apportionments are evident in Tables S17 through S19, however. Such differences appear
768 to result from ambiguities in linking PCA elements with AMS designations, different
769 numbers of factors (affecting the percentages), and differences in mean observed OA
770 (OC) concentrations. The SEARCH and AMS mean OC concentrations are comparable
771 for the CTR (SOAS) and YRK (winter) data. For JST (summer), JST (winter), and YRK
772 (summer), the mean AMS OC concentrations exceed the mean SEARCH OC

773 concentrations by 40%, 49%, and 85% respectively. The reasons for these differences are
774 unknown, but operationally could be related to sampling and analytical methods. The
775 SEARCH mean OC concentrations during the multi-week comparison periods are
776 consistent with longer-term averages from 2012, 2013, and 2008 – 2013 (Tables S17 –
777 S19). Since SEARCH reports PM_{2.5} size fractions and AMS is based on PM₁ size
778 fractions, higher AMS PM mass concentrations are not expected. No AMS component
779 appears to correspond to the PCA crustal OC, which could relate to the difference in size
780 fractions sampled. The PCA crustal OC concentrations are generally small except during
781 occasional events, as previously noted.

782 Comparisons of our results to results reported by Kleindienst et al. (2010) are shown in
783 Figure S26. Kleindienst et al. (2010) determined organic tracer concentrations on
784 archived samples from the SEARCH Carbonaceous Aerosol Characterization Experiment
785 (CACHE) archive. Twenty samples were analyzed, five each from BHM, CTR, JST, and
786 PNS, collected during May (7, 13, 22, 28) and August (17), 2005 (Kleindienst et al.,
787 2010). SEARCH OC measurements are made on filters from a sampler with a denuder
788 placed upstream to remove organic gases, whereas the CACHE sampler was not denuded.
789 The CACHE OC concentrations were ~50 – 100% higher than the SEARCH OC
790 concentrations (Figure S26), with a CACHE average OC concentration of 7.32 $\mu\text{g m}^{-3}$
791 compared with SEARCH OC average of 4.62 $\mu\text{g m}^{-3}$ when restricted to the 17 samples
792 that had both CACHE and SEARCH OC concentrations. Kleindienst et al. (2010)
793 accounted for ~70% of the measured CACHE OC concentration using 11 source types, so
794 their apportioned OC concentrations are roughly comparable to measured SEARCH OC
795 concentrations. The sum of the Kleindienst et al. (2010) diesel and wood burning OC
796 concentrations correlates highly ($r^2 = 0.83$) and agrees in magnitude (intercept = 0; slope
797 = 1) with PCA2 combustion OC (Figure S26). Wood burning OC concentrations also
798 correlate highly ($r^2 = 0.76$) with PCA2 combustion OC, corresponding to ~50 – 70% of
799 the combustion OC concentrations (Figure S26). OC_{bb} (Section 3.4) correlates less well
800 ($r^2 = 0.38$) with wood-burning OC, and OC_{bb} concentrations average ~30% higher than
801 wood-burning OC concentrations (Figure S26). As previously noted, the fixed scaling
802 factor used for estimating OC_{bb} from K_{bb} does not reflect the variability among source
803 types in OC_{bb}/K_{bb}, nor does it reflect seasonal variability in their source contributions

804 (Section 3.4). The modest correlation of OC_{bb} with organic tracer-based wood-burning
805 OC concentrations is expected due to emission source variability; overprediction of
806 wood-burning OC by OC_{bb} is expected during summer months when the principal
807 biomass burning sources (agricultural field burns, open burning of wastes) likely
808 predominate and have lower OC_{bb}/K_{bb}. The sum of the Kleindienst et al. (2010) diesel
809 and wood-burning OC concentrations correlates highly ($r^2 = 0.92$) with OC_{bb} and CO in
810 a multiple regression model (Figure S26), supporting combustion origins of OC_{bb}.

811

812 **3.5.4 Temporal variations**

813 Temporal variations of the 1999-to-2013 PCA2 results are described here primarily for
814 CTR and JST, representing (as in Table 1) one rural and one urban location having
815 extensive SEARCH data records. At JST, day-of-week variations are evident for the
816 combustion-derived OC and for the OC associated with crustal species (Figure S27),
817 consistent with the occurrence of weekly activity cycles for driving, construction, and
818 other anthropogenic emission sources. Day-of-week variations are not apparent for other
819 OC associations at JST or for any OC factors at CTR. Seasonal and SO₄-associated OC
820 exhibit pronounced monthly variations at both CTR and JST, with higher values of SO₄-
821 associated OC and of CTR seasonal OC occurring during warmer months (Figures S28
822 and S29). The patterns for CTR SO₄-associated OC (highest in July and August) and
823 seasonal OC (higher in spring and autumn than in July) are not independent.

824 Mean annual combustion-derived OC concentrations decline from 3.8 ± 0.2 to 1.4 ± 0.1
825 $\mu\text{g m}^{-3}$ between 1999 and 2013 at JST (Figures 4, S30) and from 2.9 ± 0.4 to 0.7 ± 0.1 μg
826 m^{-3} between 2001 and 2013 at BHM (not shown). Declining combustion OC
827 concentrations at the urban JST and BHM sites coincide with reductions of motor vehicle
828 emissions during this time period (Section 3.1), though these urban sites may also be
829 affected by industrial emissions. BHM additionally benefits from a decline in OC
830 associated with SO₂ from 0.4 ± 0.04 $\mu\text{g m}^{-3}$ in 2001 to 0.2 ± 0.03 $\mu\text{g m}^{-3}$ in 2013,
831 probably as a reflection of declining emissions from industrial sources within
832 Birmingham. In contrast, combustion-derived OC at CTR does not exhibit a statistically
833 significant decline, equaling 1.5 ± 0.1 $\mu\text{g m}^{-3}$ in 1999 and 1.3 ± 0.1 $\mu\text{g m}^{-3}$ in 2013

834 (Figures 4, S30). At CTR, downward OC trends are evident only for SO₄ and seasonal
835 OC (mean decreases of 0.6 μg m⁻³ and 0.7 μg m⁻³, respectively) (Figure S31). The OC
836 associated with SO₄ at CTR exhibits declines during all seasons, with the weakest such
837 change in winter (Figure S32).

838 The trend results are consistent with the combined effects of (1) regional-scale reductions
839 of ambient SO₄ and O₃ concentrations, (2) reductions of urban OC due to declining
840 mobile source OC and VOC emissions, and (3) likely predominance of biomass burning
841 OC at CTR (Hidy et al., 2014). Carbon-isotope measurements from 2004 show that fossil
842 carbon represented ~20% of CTR TC that year (Blanchard et al., 2011), indicating that
843 mobile source or other fossil fuel emissions affect CTR to some extent. Enhanced hourly
844 concentrations of EC, OC, and CO at CTR are associated with winds from the directions
845 of Birmingham, Tuscaloosa, and Montgomery (Hidy et al., 2014). EC declined by ~0.3
846 μg m⁻³ at CTR between 1999 and 2013 (Figure 1), suggesting an influence of mobile
847 source emission reductions that is possibly too modest to detect using our PCA methods
848 or is masked by annual variability in biomass burning emissions. For comparison, mean
849 EC concentrations at JST decrease by ~1.4 μg m⁻³ (Figure 1), and the overall mean EC at
850 JST (1.35 μg m⁻³) is ~4 times the overall mean EC at CTR (0.35 μg m⁻³).

851 The trends in mean annual OC from each identified species association indicate that
852 anthropogenic emission reductions decreased mean annual urban combustion OC
853 concentrations by 2.4 μg m⁻³ at JST and at BHM (and, by inference, other metropolitan
854 areas in the Southeast), and indirectly decreased SO₄ and seasonal OC by ~1.1 to 1.3 μg
855 m⁻³ throughout the southeastern U.S. between 1999 and 2013 (Figure 4). As of 2013, the
856 overall mean annual combustion-derived OC is 1.3 to 1.4 μg m⁻³ at CTR and JST,
857 whereas the sum of the mean annual SO₄ and seasonal component OC is 0.4 to 0.8 μg m⁻³
858 at CTR and JST (Figure 4).

859 **3.6 Synthesis**

860 Various apportionments of PM_{2.5} OC concentrations are presented in Sections 3.1, 3.4,
861 and 3.5. These apportionments are compared and contrasted in this section. Although the
862 apportionments utilize different methods, there is overlap of inputs. For example, Kbb is

863 used as an input in the multivariate regressions that generate “primary” organic carbon
864 (“POC”) and “secondary” organic carbon (“SOC”) (Blanchard et al., 2008, not discussed
865 here), and “POC” is a fitting species used in the CMB receptor modeling. As shown in
866 Table 5, the apportionments exhibit areas of agreement as well as certain differences.
867 Both are summarized using ratios of the values listed in Table 5. We report averages and
868 ranges across the sites.

869 Computed “POC” represents 72% (64% - 76%) of mean OC concentrations, whereas
870 “SOC” represents 29% (25% - 38%). As noted, “SOC” is the OC that is associated with
871 O₃ and SO₄, which constitutes a portion of SOA. “POC” is associated with EC, CO, and
872 K_{bb}, but may include oxidized OC that would be identified as SOA in other analyses. For
873 the CMB analysis, OC derived from area sources (primarily biomass burning), mobile
874 sources, and point sources is summed to generate combustion OC. CMB combustion OC
875 is 97% (73% - 118%) of “POC”; this level of agreement presumably is because the CMB
876 receptor model of Blanchard et. al. (2013) used “POC” as a fitting species. The largest
877 PCA1 and PCA2 OC components are combustion, seasonal, and SO₄-associated OC. The
878 sum of these three components is, for PCA1, 87% (60% - 139%) of mean measured OC
879 (the overestimate, at PNS, is balanced by negative crustal and salt components there). For
880 PCA2, the sum of combustion, seasonal, and SO₄-associated OC is 81% (58% - 101%) of
881 mean measured OC. Other PCA OC components contribute smaller amounts (Table 5).

882 PCA1 and PCA2 combustion each represent 57% (8% - 103% and 33% - 85%,
883 respectively) of CMB combustion. Other PCA factors, including SO₂, metals, and salts
884 (possibly denoting biomass burning when represented by K) may be related to specific
885 types of combustion sources.

886 These comparisons suggest that the OC_{bb} concentrations are likely biased high by ~10%
887 or more, with less evident biases at inland sites. Specifically, OC_{bb} is 99% (66% - 121%)
888 of “POC” and 109% (79% - 142%) of CMB area-source OC concentrations. At inland
889 sites, OC_{bb} is 96% (79% - 111%) of CMB area-source OC concentrations, indicating
890 approximate agreement. Although multiple analyses (OC_{bb}, “POC”, PCA2) used K_{bb} as
891 an input variable, OC_{bb} is calculated using a fixed scaling factor between OC and K_{bb}.

892 As described, uncertainty in this scaling factor is estimated to generate a factor-of-two
893 uncertainty in OC_{bb}.

894 **4 Conclusions**

895 Fifteen years of measurements of an extensive suite of gas and particle species at eight
896 SEARCH sites offer important insights into the sources of OA and the effects of
897 anthropogenic emission reductions on OA concentrations in the southeastern U.S. Five
898 analytical methods indicate that a major component (~45% on average, 1999 to 2013, all
899 sites; intersite range 25% to 63%) of OA derives from combustion sources, including
900 motor vehicles and biomass burning, at all urban and rural sites and throughout the year.
901 Reductions of emissions from combustion sources decreased overall mean annual OC
902 concentrations by $2.4 \mu\text{g m}^{-3}$ at JST and BHM (and, by inference, throughout the Atlanta
903 and Birmingham metropolitan areas) between 1999 and 2013. OA is identified partly
904 with an SO₄-OA relationship (~25% of OC, on average), which is consistent with
905 hypothesized isoprene oxidation pathways. OA is also partly identified with other
906 seasonal atmospheric processes, including atmospheric photochemical reactions (~20%
907 of OC, on average). Reductions of anthropogenic emissions of SO₂, NO_x, and VOC
908 suggest a decrease in SO₄-associated OC and seasonal-component OC concentrations by
909 $\sim 1.1 - 1.3 \mu\text{g m}^{-3}$ between 1999 and 2013 throughout the SEARCH region, implying that
910 reductions of anthropogenic emissions affect SOA concentrations.

911 As of 2013, the SEARCH mean annual combustion-derived OC concentrations are 1.3 to
912 $1.4 \mu\text{g m}^{-3}$ at CTR and JST (~60% of total OC), while the mean annual OC
913 concentrations associated with the SO₄ and seasonal components are 0.4 to $0.8 \mu\text{g m}^{-3}$ at
914 CTR and JST (~35% and ~22%, respectively). Additional attention to OC from
915 combustion emissions could yield further reductions of PM_{2.5} OC concentrations, now
916 averaging $\sim 2.5 \mu\text{g m}^{-3}$ in the southeastern U.S. Since biomass burning is a major source
917 of OC emissions in the southeastern U.S., minimizing the stated extent and timing of
918 these emissions could help improve regional air quality.

919 Additional work could improve quantitative assessments of source contributions. Carbon-
920 isotope measurements of archived SEARCH samples are in process, and will provide

921 further insight into the observed OA trends. Future research could also help define the
922 sensitivity of the SO₄-associated OC and seasonal OC to ongoing reductions of
923 anthropogenic SO₂, NO_x, and VOC emissions. Current research by many investigators is
924 better defining the role of naturally occurring VOCs, including isoprene. The SOAS and
925 SAS campaigns of June – July 2013 helped resolve uncertainties and ambiguities in OA
926 chemistry specific to that time period. Extrapolation of the short-term results to seasonal
927 and interannual time periods can be achieved through further analyses of long-term EC
928 and OC monitoring data.

929

930 **Appendix: Measurement conventions and issues**

931 Carbonaceous aerosol is conventionally divided into EC and OC, operationally defined
932 by measurement protocol, either by thermal differentiation or by light absorption (for
933 clarity, protocols based on light absorption typically report data as light-absorbing carbon
934 [LAC] or black carbon [BC], and sometimes as brown carbon [BrC], rather than as EC).
935 EC is comprised of extended aromatic rings, and is characteristically refractory,
936 insoluble, chemically inert, and light absorbing (Cappa, 2011). EC derives from
937 combustion and is believed to be exclusively from primary emission sources, including
938 motor vehicles, other transportation sources, industrial processes, and vegetation burning
939 (Chow et al., 2010; Watson et al., 2011). OC is the carbonaceous component of OA and
940 refers here to specific measurements, such as filter-based measurements made by
941 thermal-optical reflectance (TOR) (Chow et al., 2005; 2007a; 2007b). Combustion
942 sources that emit EC also emit OC.

943 Organic compounds that are directly emitted in the condensed phase are typically
944 identified as POA, whereas SOA commonly refers to organic material transferring from
945 gases to the condensed phase through chemical transformation (Kanakidou et al., 2005).
946 Gases of varying degrees of volatility may be oxidized and incorporated into the
947 condensed phase (Robinson et al., 2007; Huffman et al., 2009). Chemical reactions may
948 take place in the condensed phase in the presence of water, and partitioning by phase are
949 key elements of uncertainty in describing SOA (e.g., Carlton and Turpin, 2013; Nguyen
950 et al., 2015; Isaacman-VanWertz et al., 2015). Atmospheric chemical reactions involving

951 VOCs (Hallquist et al., 2009), especially including compounds of intermediate volatility
952 (de Gouw et al., 2011), are known to generate oxygenated reaction products on time
953 scales of minutes to days. Secondary organic species may be associated with other
954 secondary species, such as O₃ or SO₄, either through a common driver of photochemical
955 oxidation processes or due to direct chemical relationships; this is an active area of
956 research.

957 The initial aging of fresh, concentrated emissions begins with turbulent dilution seconds
958 after hot exhaust effluent enters into the cooler atmosphere. Fine particle evolution then
959 takes place more slowly over nominal ~5-7 day lifetimes as particles are mixed and
960 transported, and lost by deposition. These processes are often referred to as “aging” of a
961 freshly emitted aerosol. The aging processes can be chemical in nature, or may involve
962 physical processes as well, including absorption in clouds or precipitation followed by
963 hydrometeor evaporation.

964 The exceptions to the definition of SOA as material transferring from gas to condensed
965 phases through chemical transformation include: (1) volatile or semi-volatile material that
966 condenses into aerosol without undergoing chemical transformation (Kanakidou et al.,
967 2005), (2) gases absorbed into hydrometeors, leaving residual aerosol on evaporation,
968 which might be understood as either POA or SOA depending on absence or occurrence of
969 chemical transformation (Kanakidou et al., 2005), and (3) material emitted in the
970 condensed phase that undergoes chemical transformation, possibly shifting multiple times
971 between gas and aerosol, and that appears as oxidized compounds on analysis of aerosol
972 samples (Donahue et al., 2009). The last exception is especially ambiguous: such material
973 may be classified as POA in an emission inventory, but be identified as SOA according to
974 measurements designated as “more oxygenated aerosol (OOA)” by aerosol mass
975 spectrometry (AMS).

976 Dilution sampling is routinely used to characterize exhaust emissions because it yields
977 estimates of EC and OC at temperatures characteristic of the ambient atmosphere, but
978 further phase exchange of POA may be expected in the real world with ongoing dilution.
979 Photochemical chamber studies demonstrate that organic aerosol from hot exhaust
980 emissions (e.g., diesel engine exhaust) shifts from POA to SOA dominance typically

981 within one or more hours of photo-oxidation (Presto et al., 2014). The comparability of
982 POA measurements from such studies to emission inventory estimates of mobile source
983 PM is poorly characterized. For modeling, a volatility basis set (VBS) provides more
984 realistic diluted emission estimates by recognizing that POA spans a range of volatilities,
985 and cannot be treated as entirely nonvolatile (Robinson et al., 2007; Donahue et al., 2009;
986 Donahue et al., 2012).

987 The mass concentrations of EC are approximately conserved from emission sources to
988 receptor sites, whereas losses due to volatilization of certain PM_{2.5} organic compounds
989 readily occur. OA concentrations may increase as SOA forms not only from POA
990 vaporization, subsequent reactions and condensation, but also, perhaps predominantly,
991 from atmospheric reactions of gas-phase precursors. Organic mass (OM), which includes
992 not only carbon but also other atoms (e.g., oxygen and hydrogen) that are components of
993 OA, is not conserved. There is no accepted measure of aging in atmospheric aerosols, but
994 some workers have adopted OM/OC as an indicator. As POA ages, the ratio of oxygen-
995 to-carbon typically increases, increasing the mass of OM. Aerosol aging can, therefore,
996 increase both the OM/EC ratio and the OC/EC ratio (by definition, EC concentrations are
997 not expected to increase with the formation of species during aging). A graphical
998 depiction of various categorizations of OA is shown in the supplement (Figure S1).

999 Receptor-modeling methods have identified POA source types using measurements of
1000 conservative organic tracer species (Schauer et al., 1996), indicating that motor vehicles
1001 contribute ~ 2 to 4 $\mu\text{g m}^{-3}$ to annual-average OC concentrations in Atlanta (e.g., Zheng et
1002 al. 2002; 2006). SEARCH thermal desorption-gas chromatograph mass spectrometer
1003 (TD-GC/MS) measurements suggest that 30 to 50% of the observed 2006 to 2010 OC
1004 trend in Atlanta, Georgia and Birmingham, Alabama could be due to changes in mobile
1005 source emissions (Blanchard et al., 2014a). These trends need not be entirely from
1006 changes in POA emissions; diesel SOA, for example, is an important component of
1007 mobile source OA (Presto et al., 2014), and is linked to EC and POA emissions. Aside
1008 from motor vehicle exhaust, biomass burning is a major source of EC and the largest
1009 source of OC emissions in the southeastern U.S. according to emission inventories, with
1010 little evidence for substantial trend between 1999 and 2013 (Hidy et al., 2014). Carbon-

1011 isotope (^{14}C) measurements at SEARCH sites indicate that on average 2 to 4 $\mu\text{g m}^{-3}$ of
1012 OC is modern in origin (rural and urban sites), with ~40% fossil in Atlanta and ~60%
1013 fossil in Birmingham during 2004 and 2005 (Blanchard et al., 2011). Together, the
1014 measurements suggest the presence of a large modern-carbon contribution added to
1015 downward-trending mobile source contributions (Hidy et al., 2014).

1016 Significant emissions of VOC from vegetation, including isoprene and terpenes, occur in
1017 the southeastern U.S. and represent a major, and possibly a dominant, source of SOA
1018 (Goldstein et al., 2009). Although incompletely quantified, SOA derived from
1019 anthropogenic and biogenic VOC products has been estimated to be ~20 to 60% of the
1020 OA observed in the southeastern U.S. (Table S1), varying among samples and especially
1021 by season (Lim and Turpin, 2002; Zheng et al., 2006; Saylor et al., 2006; Blanchard et
1022 al., 2008). Field and laboratory work over the years has refined the chemical pathways,
1023 with evidence for both aqueous and gas-phase chemistry. Ground-level filter samples
1024 from southeastern sites have yielded expected tracers of SOA-formation chemistry from
1025 biogenic precursors (Gao et al., 2006; Surratt et al., 2007; Chan et al., 2010; Hatch et al.,
1026 2011a; 2011b). The presence of naturally occurring VOCs, modulated by temperature
1027 and solar radiation, is expected to be roughly constant over a period of years, suggesting
1028 a near constant level of biogenic SOA. However, isoprene concentrations appear to have
1029 increased at Atlanta-area sites between 2002 and 2012 (Hidy et al., 2014); the reason for,
1030 and significance of, this trend for SOA trends in the Southeast is unclear. Interaction of
1031 biogenic and anthropogenic emissions potentially affect SOA formation (Weber et al.,
1032 2007; Shilling et al., 2012; Xu et al., 2015a), so biogenic SOA trends could result from
1033 anthropogenic emission reductions.

1034 Determination of the fraction of OC not directly attributed to sources is complicated by
1035 both the influence of atmospheric processes on emissions and the methods of
1036 measurement of OC or its components. The processing of atmospheric aerosols is
1037 exceedingly complex as a result of the chemistry of volatile and non-volatile carbon
1038 emissions and interactions between chemical and meteorological processes on multiple
1039 time and space scales. Advancing knowledge about the SOC component has been
1040 inhibited by the lack of chemical detail in long-term observations and the short-term

1041 application of more recent measurement methods. Measurements of atmospheric organic
1042 carbon as POC and SOC refer to operational definitions, including those in Figure S1.
1043 Historically, measurements of OC and EC have relied on filter sampling and subsequent
1044 analysis for OC constituents in the laboratory. The filter sampling and recently
1045 introduced continuous methods provide different data for EC and OC as well as some
1046 identification of constituents resolved in space in time. However, their quantitative
1047 comparison remains problematic as indicated in this study. Continuing research,
1048 including method comparisons, and expanded detailed atmospheric observations will be
1049 required to resolve these uncertainties.

1050

1051 **Author contributions**

1052 C. L. B., G. M. H., S. S., K. B., and E. S. E. designed the study. E. S. E. and K. B.
1053 operated the measurement program and prepared the data sets. C. L. B. carried out the
1054 statistical analyses. C. L. B. and G. M. H. wrote the manuscript with contributions from
1055 all co-authors.

1056

1057 **Acknowledgements**

1058 The authors thank J. Jansen, E. Knipping, and the ARA staff for their contributions to this
1059 work. Funding for the SEARCH network has come from Southern Company and the
1060 Electric Power Research Institute. We are indebted to these sponsors for supporting this
1061 unique long-term measurement program.

1062

1063

1064 **References**

- 1065 Andreae, M.O. and Merlet, P.: Emission of trace gases and aerosols from biomass
1066 burning, *Global Biogeochem. Cy.*, 15 (4), 955-966, 2001.
- 1067 Andreae, M.O., Atlas, E., Cachier, H., Cofer III, W.R., Harris, G. W., Helas, G.,
1068 Koppmann, R., Lacaux, J.-P., and Ward, D.E.: Trace gas and aerosol emissions from
1069 savanna fires, in: Levine, J.S., ed., *Biomass Burning and Global Change*, MIT Press,
1070 Cambridge MA, 278-295, 1996.
- 1071 Atmospheric Research and Analysis (ARA), [http://www.atmospheric-](http://www.atmospheric-research.com/studies/SEARCH/index.html)
1072 [research.com/studies/SEARCH/index.html](http://www.atmospheric-research.com/studies/SEARCH/index.html), last access 10 July 2014.
- 1073 Baumann, K., Flanagan, J.B., and Jayanty, R.K.M.: Fine particulate matter source
1074 apportionment for the chemical Speciation Trends Network site at Birmingham,
1075 Alabama, using Positive Matrix Factorization, *J. Air Waste Manage.*, 58, 27-44, 2008.
- 1076 Blanchard, C. L., Hidy, G. M., Tanenbaum, S., Edgerton, E., Hartsell, B., and Jansen, J.:
1077 Carbon in southeastern aerosol particles: empirical estimates of secondary organic
1078 aerosol formation, *Atmos. Environ.*, 42, 6710-6720, 2008.
- 1079 Blanchard, C. L., Hidy, G. M., and Tanenbaum, S.: NMOC, ozone, and organic aerosol in
1080 the southeastern states, 1999-2007: 1. Spatial and temporal variations of NMOC
1081 concentrations and composition in Atlanta, Georgia, *Atmos. Environ.*, 44, 4827-4839
1082 doi:10.1016/j.atmosenv.2010.08.036, 2010.
- 1083 Blanchard, C. L., Hidy, G. M., and Tanenbaum, S.: NMOC, ozone, and organic aerosol in
1084 the southeastern states, 1999-2007: 3. Origins of organic aerosol in Atlanta, Georgia,
1085 and surrounding areas, *Atmos. Environ.*, 45, 1291-1302,
1086 doi:10.1016/j.atmosenv.2010.12.004, 2011.
- 1087 Blanchard, C. L., Tanenbaum, S., and Hidy, G. M.: Source attribution of air pollutant
1088 concentrations and trends in the Southeastern Aerosol Research and Characterization
1089 (SEARCH) network, *Environ. Sci. Technol.*, dx.doi.org/10.1021/es402876s, 2013.
- 1090 Blanchard, C. L., Chow, J., Edgerton, E., Watson, J.G., Hidy, G. M., and Shaw, S.:
1091 Organic aerosols in the southeastern United States: speciated particulate carbon

1092 measurements from the SEARCH network, 2006-2010, *Atmos. Environ.*, 95, 327-333,
1093 dx.doi.org/10.1016/j.atmosenv.2014.06.050, 2014a.

1094 Blanchard, C. L., Tanenbaum, S., and Hidy, G. M.: Spatial and temporal variability of air
1095 pollution in Birmingham, Alabama, *Atmos. Environ.*,
1096 [doi:10.1016/j.atmosenv.2014.01.006](http://dx.doi.org/10.1016/j.atmosenv.2014.01.006), 2014b.

1097 Bougiatioti, A., Stavroulas, I., Kostenidou, E., Zarmpas, P., Theodosi, C., Kouvarakis,
1098 G., Canonaco, F., Prévôt, A. S. H., Nenes, A., Pandis, S. N., and Mihalopoulos, N.:
1099 Processing of biomass burning aerosol in the eastern Mediterranean during
1100 summertime, *Atmos. Chem. Phys.*, 14, 4793–4807, [www.atmos-chem-](http://www.atmos-chem-phys.net/14/4793/2014/)
1101 phys.net/14/4793/2014/, [doi:10.5194/acp-14-4793-2014](http://dx.doi.org/10.5194/acp-14-4793-2014), 2014.

1102 Budisulistiorini, S., Canagaratna, R., Croteau, P., Marth, W., Baumann, K., Edgerton, E.,
1103 Show, S., Knipping E., Worsnop, D., Jayne, J., Gold, A., and Surratt, J.: Real-time
1104 continuous characterization of secondary organic aerosol derived from isoprene
1105 epoxydiols in downtown Atlanta, Georgia, using the Aerodyne Chemical Speciation
1106 Monitor, *Environ. Sci. Technol.*, 47, 5686-5694, 2013.

1107 Budisulistiorini, S. H., Li, X., Bairai, S. T. , Renfro, J., Liu, Y., Liu, Y. J. , McKinney,
1108 K., Martin, S. T., McNeill, V. F., Pye, H. O. T., Neff, M. , Stone, E. A., Mueller, S.,
1109 Knote, C., Shaw, S. L., Zhang, Z., Gold, A., and Surratt, J. D.: Examining the effects of
1110 anthropogenic emissions on isoprene-derived secondary organic aerosol formation
1111 during the 2013 Southern Oxidant and Aerosol Study (SOAS) at the Look Rock,
1112 Tennessee, ground site, *Atmos. Chem. Phys. Discuss.* 15, 7365-7417,
1113 [doi:10.5194/acpd-15-7365-2015](http://dx.doi.org/10.5194/acpd-15-7365-2015), 2015.

1114 Calloway, C. P., Li, S., Buchanan, J. W., and Stevens, R. K.: A refinement of the
1115 potassium tracer method for residential wood smoke, *Atmos. Environ.*, 23, 67-69, 1989.

1116 Cappa, C.: Measurements of Aerosol Carbon in the Atmosphere, AAAR Tutorial, 3
1117 October 2011, AAAR 30th Annual Conference, October 3 – 7, 2011, Orlando, FL,
1118 <http://aar.conference2011.org/content/tutorials>, last access 22 May 2014, 2011.

1119 Carlton, A. and Turpin, B.: Particle partitioning potential of organic compounds is
1120 highest in the Eastern US and driven by anthropogenic water, *Atmos. Chem. Phys.*, 13,
1121 10203-102114, 2013.

1122 Chan, M. N., Surratt, J. D., Claeys, M., Edgerton, E. S., Tanner, R. L., Shaw, S. L.,
1123 Zheng, M., Knipping, E. M., Eddingsaas, N. C., Wennberg, P. O., and Seinfeld, J. H.:
1124 Characterization and quantification of isoprene-derived epoxydiols in ambient aerosol
1125 in the southeastern United States, *Environ. Sci. Technol.*, 44, 4590–4596, 2010.

1126 Chow, J., Watson, J., Kuhns, H., Etyemezian, V., Lowenthal, D., Crow, D., Kohl, S.,
1127 Engelbrecht, J., and Green, M.: Source profiles for industrial, mobile and area sources
1128 in the Big Bend Regional Aerosol Visibility and Observational Study, *Chemosphere*,
1129 54, 185-208, 2004.

1130 Chow, J. C., Watson, J. G., Chen, L.-W. A., Paredes-Miranda, G., Chang, M.-C. O.,
1131 Trimble, D. L., Fung, K. K., Zhang, H., and Yu, J. Z.: Refining temperature measures
1132 in thermal/optical carbon analysis, *Atmos. Chem. Phys.* 5(4), 2961-2972, 1680-
1133 7324/acp/2005-5-2961, [http://www.atmos-chem-phys.net/5/2961/2005/acp-5-2961-](http://www.atmos-chem-phys.net/5/2961/2005/acp-5-2961-2005.pdf)
1134 2005.pdf, last access 22 May 2015, 2005.

1135 Chow, J. C., Watson, J. G., Chen, L.-W. A., Chang, M. C. O., Robinson, N. F., Trimble,
1136 D. L., and Kohl, S. D.: The IMPROVE_A temperature protocol for thermal/optical
1137 carbon analysis: Maintaining consistency with a long-term database, *J. Air Waste*
1138 *Manage.*, 57(9), 1014-1023, 2007a.

1139 Chow, J. C., Yu, J. Z., Watson, J. G., Ho, S. S. H., Bohannan, T. L., Hays, M. D., and
1140 Fung, K. K.: The application of thermal methods for determining chemical composition
1141 of carbonaceous aerosols: a review, *J. Environ. Sci. Heal. A*, 42(11), 1521-1541, 2007b.

1142 Chow, J.C., Watson, J.G., Lowenthal, D.H., Chen, L.-W.A., and Motallebi, N.: Black and
1143 organic carbon emission inventories: review and application to California, *J. Air Waste*
1144 *Manage.*, 60(4), 497-507, [http://www.tandfonline.com/doi/pdf/10.3155/1047-](http://www.tandfonline.com/doi/pdf/10.3155/1047-3289.60.4.497)
1145 3289.60.4.497, last access 22 May 2015, 2010.

1146 Dattner, S. and Hopke, P., eds.: Receptor Models Applied to Contemporary Pollutions
1147 Problems: Proceedings of a Specialty Conference, Air Pollution Control Association,
1148 Publishers Choice Book Manufacturing Co., Mars, Pennsylvania, 368 pp, 1982.

1149 de Gouw, J. A., Middlebrook, A. M., Warneke, C., Ahmadov, R., Atlas, E. L., Bahreini,
1150 R., Blake, D. R., Brock, C. A., Brioude, J., Fahey, D. W., Fehsenfeld, F. C., Holloway,
1151 J. S., Le Henaff, M., Lueb, R. A., McKeen, S. A., Meagher, J. F., Murphy, D. M., Paris,
1152 C., Parrish, D. D., Perring, A. E., Pollack, I. B., Ravishankara, A. R., Robinson, A. L.,
1153 Ryerson, T. B., Schwarz, J. P., Spackman, J. R., Srinivasan, A., and Watts, L. A.:
1154 Organic aerosol formation downwind from the Deepwater Horizon oil spill, *Science*,
1155 331, 1295-1299, doi:10.1126/science.1200320, 2011.

1156 Ding, X., Zheng, M., Edgerton, E., Jansen, J., and Wang, X.: Contemporary or fossil
1157 origin: Split of estimated secondary organic carbon in the southeastern United States,
1158 *Environ. Sci. Technol.*, 42, 9122-9128, 2008.

1159 Donahue, N. M., Robinson, A. L., and Pandis, S. N.: Atmospheric organic particulate
1160 matter: from smoke to secondary organic aerosol, *Atmos. Environ.*, 43, 94–106,
1161 doi:10.1016/j.atmosenv.2008.09.055, 2009.

1162 Donahue, N. M., Kroll, J. H., Robinson, A. L., Pandis, S. N., and Robinson, A. L.: A two-
1163 dimensional volatility basis set – part 2: diagnostics of organic-aerosol evolution,
1164 *Atmos. Chem. Phys.*, 12, 615–634, doi:10.5194/acp-12-615-2012, www.atmos-chem-
1165 phys.net/12/615/2012/, last access 22 May 2015, 2012.

1166 Edgerton, E. S., Hartsell, B. E., Saylor, R. D., Jansen, J. J., Hansen, D. A., and Hidy, G.
1167 M.: The Southeastern Aerosol Research and Characterization Study: part 2 – filter-
1168 based measurements of PM_{2.5} and PM_{coarse} mass and composition, *J. Air Waste*
1169 *Manage.*, 55, 1527-1542, 2005.

1170 Edgerton, E. S., Hartsell, B. E., Saylor, R. D., Jansen, J. J., Hansen, D. A., and Hidy, G.
1171 M.: The Southeastern Aerosol Research and Characterization Study, part 3: continuous
1172 measurements of fine particulate matter mass and composition, *J. Air Waste Manage.*,
1173 56, 1325-1341, 2006.

1174 Gao, S., Surratt, J., Knipping, E., Edgerton, E., Shahgholi, M., and Seinfeld, J.:
1175 Characterization of polar organic compounds in fine aerosols in the southeastern United
1176 States: identity, origin and evolution, *J. Geophys. Res.*, 111, doi
1177 10.1029/2005JD006601, 2006.

1178 Goldstein, A. H., Koven, C. D., Heald, C. L., and Fung, I. Y.: Biogenic carbon and
1179 anthropogenic pollutants combine to form a cooling haze over the southeastern United
1180 States, *P. Natl. Acad. Sci. USA*, 106, 8835-8840, doi: 10.1073/pnas.0904128106, 2009.

1181 Guo, H., Xu, L., Bougiatioti, A., Cerully, K. M., Capps, S. L., Hite Jr., J. R., Carlton, A.
1182 G., Lee, S.-H., Bergin, M. H., Ng, N. L., Nenes, A., and Weber, R. J.: Fine-particle
1183 water and pH in the southeastern United States, *Atmos. Chem. Phys.*, 15, 5211–5228,
1184 2015.

1185 Haines, T.K., Busby, R.L., and Cleaves, D.A.: Prescribed burning in the South: trends,
1186 purpose, and barriers, *South. J. Appl. For.*, 25, 149-153, 2001.

1187 Hallquist, M., Wenger, J. C., Baltensperger, U., Rudich, Y., Simpson, D., Claeys, M.,
1188 Dommen, J., Donahue, N. M., George, C., Goldstein, A. H., Hamilton, J. F.,
1189 Herrmann, H., Hoffmann, T., Iinuma, Y., Jang, M., Jenkin, M. E., Jimenez, J. L.,
1190 Kiendler-Scharr, A., Maenhaut, W., McFiggans, G., Mentel, Th. F., Monod, A.,
1191 Prévôt, A. S. H., Seinfeld, J. H., Surratt, J. D., Szmigielski, R., and Wildt, J.: The
1192 formation, properties and impact of secondary organic aerosol: current and emerging
1193 issues, *Atmos. Chem. Phys.*, 9, 5155–5236, 2009.

1194 Hand, J., Schichtel, B., Pitchford, M., Malm, W., and Frank, N.: Seasonal composition of
1195 remote and urban fine particulate matter in the United States, *J. Geophys. Res. Atmos.*
1196 117, D05209, doi:10.1029/2011JD 017122, 2012.

1197 Hansen, D.A., Edgerton, E. S., Hartsell, B. E., Jansen, J. J., Hidy, G. M., Kandasamy, K.,
1198 and Blanchard, C. L.: The Southeastern Aerosol Research and Characterization Study
1199 (SEARCH): 1. overview, *J. Air Waste Manage.*, 53, 1460-1471, 2003.

1200 Hatch, L. E., Creamean, J. M., Ault, A. P., Surratt, J. D., Chan, M. N., Seinfeld, J. H.,
1201 Edgerton, E. S., Su, Y., and Prather, K. A.: Measurements of isoprene-derived
1202 organosulfates in ambient aerosols by aerosol time-of-flight mass spectrometry, part 1:

1203 single particle atmospheric observations in Atlanta, *Environ. Sci. Technol.*, 45(12),
1204 5105–5111, 2011a.

1205 Hatch, L. E., Creamean, J. M., Ault, A. P., Surratt, J. D., Chan, M. N., Seinfeld, J. H.,
1206 Edgerton, E. S., Su, Y., and Prather, K. A.: Measurements of isoprene-derived
1207 organosulfates in ambient aerosols by aerosol time-of-flight mass spectrometry, part 2:
1208 temporal variability & formation mechanisms, *Environ. Sci. Technol.*, 45 (20), 8648–
1209 8655, 2011b.

1210 Hidy, G. M., Blanchard, C.L, Baumann, K, Edgerton, E., Tanenbaum, S., Shaw, S.,
1211 Knipping, E., Tombach, I., Jansen, J. J., and Walters, J.: Chemical climatology of the
1212 southeastern United States, 1999 – 2013, *Atmos. Chem. Phys.*, 14, 11893–11914,
1213 doi:10.5194/acp-14-11893-2014, 2014.

1214 Hobbs, H, Reid, J.S., Herring, J.A., Nance, J. D., Weiss, R. E, Ross, J. L., Hegg, D. A.,
1215 Ottmar, R. D., and Liousse, C.: Particle and trace-gas measurements in the smoke from
1216 prescribed burns of forest products in the Pacific northwest, in: Levine, J.S., ed.,
1217 *Biomass Burning and Global Change*, MIT Press, Cambridge MA, 607-715, 1996.

1218 Hu, W., Campuzano-Jost, P., Palm, B., DSay, D., Ortega, A., Hayes, P., Krechner, J.,
1219 Chen, Q, Kuwata, M., Liu, Y., De Sa, S., Martin, S., Hum, M., Budisulistiorini, S., Riva,
1220 M., Surratt, J., St. Clair, J., Isaacman-VanWertz, G., Yee, L., Goldstein, A., Carbone,
1221 S., Artaxo, P., DeGouw, J., Koss, A., Wisthaler, A., Mikoviny, T., Karl, T., Kaser, L.,
1222 Jud, W., Hansel, A., Docherty, K., Robinson, N., Coe, H., Allan, J., Canagaratna, M.,
1223 Paulot, F., and Jimenez, J.: Characterization of a real-time tracer for isoprene
1224 epoxidiols-derived secondary organic (IEPOX-SOA) from aerosol mass spectrometer
1225 measurements, *Atmos. Chem. Phys. Discuss.*, 15, 11223-11276, 2015.

1226 Huffman, J. A., Docherty, K. S., Mohr, C., Cubison, M. J., Ulbrich, I. M., Ziemann, P. J.,
1227 Onasch, T. B., and Jimenez, J. L.: Chemically-resolved volatility measurements of
1228 organic aerosol from different sources, *Environ. Sci. Technol.*, 43, 5351–5357, 2009.

1229 Isaacman-VanWertz, G., Goldstein, A., Yee, L., Kreisberg, N., Wernis, R., Moss, J.,
1230 Hering, S., de Sa, S., Martin, S., Alexander, L., Palm, B., Hu, W., Campuzano-Jost, P.,
1231 Day, D., Jimenez, J., Riva, M., Surratt, J., Edgerton, E., Baumann, K., Viegas, J.,

1232 Manzi, A., deSouza, R., and Artaxo, P.: Biogenic oxidation products that dominate
1233 secondary organic aerosol in forested environments actively partitioning between gas
1234 and particle phases, in preparation, 2015.

1235 Kanakidou, M., Seinfeld, J. H., Pandis, S. N., Barnes, Dentener, F. J., Facchini, M. C.,
1236 Van Dingenen, R., Ervens, B., Nenes, A., Nielsen, C. J., Swietlicki, E., Putaud, J. P.,
1237 Balkanski, Y., Fuzzi, S., Horth, J., Moortgat, G. K., Winterhalter, R., Myhre, C. E. L.,
1238 Tsigaridis, K., Vignati, E., Stephanou, E. G., and Wilson, J.: Organic aerosol and global
1239 climate modelling: a review, *Atmos. Chem. Phys.*, 5, 1053–1123, [www.atmos-chem-](http://www.atmos-chem-phys.org/acp/5/1053/)
1240 [phys.org/acp/5/1053/](http://www.atmos-chem-phys.org/acp/5/1053/), last access 2 September 2014, 2005.

1241 Kim, P., Jacob, D., Fisher, J., Travis, K., Yu, K., Zhu, L., Yantosca, R., Sulprizio,
1242 Jiminez, J., Campusano-Jost, P., Froyd, K., Liao, J., Hair, J., Fenn, M., Butle, C.,
1243 Wagner, N., Gordon, T., Welti, A., Wennberg, P., Crounsem J., St. Clair, j., Teng, A.,
1244 Millet, D., Schwarz, J., Markovic, M., and Perring, A.: Sources, seasonality and trends
1245 of Southeast US aerosol: an integrated analysis of surface, aircraft, and satellite
1246 observations with the GEOS-CHEM chemical transport model, *Atmos. Chem. Phys.*
1247 *Discuss.*, 15, 17651-17709, 2015.

1248 Kleindienst, T., Jaoui, M., Lewandowski, M., Offenburg, J., Lewis, C., Bhave, P., and
1249 Edney, E.: Estimates of the contribution of biogenic and anthropogenic hydrocarbons to
1250 secondary organic aerosol at a southeastern US location, *Atmos. Environ.*, 41, 8288-
1251 8300, 2007.

1252 Kleindienst, T., Lewandowski, M., Offenburg, J., and Edney, E.: Contribution of primary
1253 and secondary sources of organic aerosol and PM_{2.5} at SEARCH network sites, *J. Air*
1254 *Waste Manage. Assoc.*, 60, 1388-1399, 2010.

1255 Kroll, J., Ng, N., Murphy, S., Flagan, R., and Seinfeld, J.: Secondary organic aerosol
1256 formation from isoprene photooxidation, *Environ. Sci. Technol.*, 40, 1869-1877, 2006.

1257 Landis, M.S., Lewis, C. W., Stevens, R. K., Keeler, G. J., Dvonch, J. T., and Tremblay,
1258 R. T.: Ft. McHenry tunnel study: source profiles and mercury emissions from diesel
1259 and gasoline powered vehicles, *Atmos. Environ.*, 41, 8711–8724,
1260 [doi:10.1016/j.atmosenv.2007.07.028](https://doi.org/10.1016/j.atmosenv.2007.07.028), 2007.

1261 Lee, S., Baumann, K., Schauer, J. J., Sheesley, R. J., Naeher, L. P., Meinardi, S., Blake,
1262 D. R., Edgerton, E. S., Russell, A. G., and Clements, M.: Gaseous and particulate
1263 emissions from prescribed burning in Georgia, *Environ. Sci. Technol.*, 39, 9049-9056,
1264 2005.

1265 Lee, D., Balachandran, S. Pachon, J., Shankaran, R., Lee, S., Mulholland, J. A., and
1266 Russell, A. G. Ensemble-trained PM_{2.5} source apportionment approach for health
1267 studies. *Environ. Sci. Technol.*, 43, 7023–7031, 2009.

1268 Lewandowski, M., Piletic, I., Kleindienst, T., Offenburg, J., Beaver, M., Jaoui, M.,
1269 Docherty, K., and Edney, E.: Secondary organic aerosol characterization at field sites
1270 across the United States during the spring-summer period, *Intern J. Environ. Anal.*
1271 *Chem.* 93, 1084-1103, 2013.

1272 Lewis, C. W.: Determining the sources of particulate and VOC pollutants in ambient air
1273 by radiocarbon (¹⁴C) measurements, Sixth International Conference, Preservation of
1274 Our World in the Wake of Change, Jerusalem, June 30 – July 4, 1996.

1275 Lewis, C. W., Baumgardner, R. E., and Stevens, R. K.: Contribution of woodsmoke and
1276 motor vehicle emissions to ambient aerosol mutagenicity, *Environ. Sci. Technol.*, 22,
1277 968-971, 1988.

1278 Lewis, C. W., Norris, G. A., Conner, T. L., and Henry, R. C.: Source apportionment of
1279 Phoenix PM_{2.5} aerosol with the UNMIX receptor model, *J. Air Waste Manage.*, 53, 325
1280 – 338, doi: 10.1080/10473289.2003.10466155, 2003.

1281 Lewis, C., Klouda, G., Ellenson, W.: Radiocarbon measurement of the biogenic
1282 contribution to summertime PM-2.5 ambient aerosol in Nashville, TN, *Atmos. Environ.*
1283 38, 6053-6061, 2004.

1284 Liao, J., Froyd, K., Murphy, D., Keutsch, F., Yu, G., Wennberg, P., St. Clair, J., Crounse,
1285 J., Wisthaler, A., Mikoviny, T., Jiminez, J., Campuzano-Jost, P., Day, D., Hu, W.,
1286 Ryerson, T., Pollack I., Peischl, J., Anderson, B., Ziemba, L., Blacke, D., Meinhardi, S.,
1287 and Diskin, G.: Airborne measurements of organosulfates over the continental U.S., *J.*
1288 *Geophys. Res. Atmos.*, 120, doi:10.1002/so14JD022378, 2015.

1289 Lim, H. and Turpin, B.: Origins of primary and secondary organic aerosol in Atlanta:
1290 results of time-resolved measurements during the Atlanta Supersite experiment,
1291 Environ. Sci. Technol., 36, 4489-4496, 2002.

1292 Lin, Y., Knipping, E., Edgerton, E., Shaw, S., and Surratt, J.: Investigating the influences
1293 of SO₂ and NH₃ levels on isoprene-derived secondary organic aerosol formation using
1294 conditional sampling approaches, Atmos. Chem. Phys., 13, 8457-8470, 2013.

1295 Lin, Y., Budisulistiorini, S., Chu, K., Siejack, R., Zhang, H., Riva, M., Zhang, Z., Gold,
1296 A., Kautzman, K., and Surratt, J.: Light-absorbing oligomer formation in secondary
1297 organic aerosol from reactive uptake of isoprene epoxidiols, Environ. Sci. Technol., 48,
1298 12012-12021, 2014.

1299 Malm, W.C., Day, D., Kreidenweis, S., Collett, J., Carrico, C., McMeeking, G., and Lee,
1300 T.: Hygroscopic properties of an organic-laden aerosol, Atmos. Environ., 39, 4969-
1301 4982, 2005.

1302 Taylor, N., Collins, D., Spencer, C., Lowenthal, D., Zielenska, B., Samburova, V., and
1303 Kumar, N.: Measurement of ambient aerosol hydration state at Great Smoky Mountains
1304 National Park in the southeastern United States, Atmos. Chem. Phys., 11, 12085-2011,
1305 doi:10.5194/acp-1112085-2011, 2011.

1306 May, A., Saleh, R., Hennigan, C., Donahue, N., and Robinson, A.: Volatility of organic
1307 molecular markers used for source apportionment analysis: measurements and
1308 implications for atmospheric lifetime, Environ. Sci. Technol., 46, 12435-12444, 2012.

1309 McDonald, J. D., Chow, J. C., Peccia, J., Liu, Y., Chand, R., Hidy, G. M., and Mauderly,
1310 J. L.: Influence of collection region and site type on the composition of paved road
1311 dust, Air Qual Atmos Heal, 6, 615–628, doi 10.1007/s11869-013-0200-4, 2013.

1312 McDonald, B., Goldstein, A., and Harley, R.: Long-term trends in California mobile
1313 source emissions and ambient concentrations of black carbon and organic aerosol,
1314 Environ. Sci. Technol., 49, 5178-5188, 2015.

1315 Murphy, B. and Pandis, S.: Exploring summertime organic aerosol formation in the
1316 eastern United States using a regional-scale budget approach and ambient

1317 measurements, *J. Geophys. Res. Atmos.* 115, D24216, doi:10.1029/2010JD14418,
1318 2010.

1319 Nguyen, E. R., Capps, S., and Carlton, A.: Decreasing aerosol water with OC trends in
1320 the southeast U.S., *Environ. Sci. Technol.* 49, 7843-7850, 2015.

1321 Pachon, J. E., Balachandran, S., Hu, Y., Weber, R. J., Mulholland, J. A., and Russell, A.
1322 G.: Comparison of SOC estimates and uncertainties from aerosol chemical composition
1323 and gas phase data in Atlanta, *Atmos. Environ.*, 44, 3907-3914, 2010.

1324 Pachon, J. E., Weber, R. J., Zhang, X., Mulholland, J. A., and Russell, A. G. Revising the
1325 use of potassium (K) in the source apportionment of PM_{2.5}, *Atmos. Pollut. Res.*, 4, 14 –
1326 21, 2013.

1327 Pandis, S., Paulson, S., Seinfeld, J., and Flagan, R.: Aerosol formation in the
1328 photooxidation of isoprene and b-pinene, *Atmos. Environ.* 25A, 1997-1991, 1991.

1329 Presto, A. A., Gordon, T. D., and Robinson, A. L.: Primary to secondary organic aerosol:
1330 evolution of organic emissions from mobile combustion sources, *Atmos. Chem. Phys.*,
1331 14, 5015–5036, doi:10.5194/acp-14-5015-2014, [www.atmos-chem-](http://www.atmos-chem-phys.net/14/5015/2014/)
1332 [phys.net/14/5015/2014/](http://www.atmos-chem-phys.net/14/5015/2014/), last accessed 2 September 2014, 2014.

1333 Provencher, L., Herring, B. J., Gordon, D. R., Rodgers, H. L., Tanner, G. W., Hardesty, J.
1334 L., Brennan, L. A., and Litt, A. R.: Longleaf pine and oak responses to hardwood
1335 reduction techniques in fire-suppressed sandhills in northwest Florida, *Forest Ecol.*
1336 *Manag.*, 148, 63-77, 2001.

1337 Reff, A., Bhave, P., Simon, H., Pace, T. S., Pouliot, G. A., Mobley, D., and Houyoux, M.:
1338 Emissions inventory of PM_{2.5} trace elements across the United States, *Environ. Sci.*
1339 *Technol.*, 43, 5790–5796, 2009.

1340 Reid, J. S., Koppmann, R., Eck, T. F., and Eleuterio, D. P.: A review of biomass burning
1341 emissions part II: intensive physical properties of biomass burning particles, *Atmos.*
1342 *Chem. Phys.*, 5, 799–825, [http://www.atmos-chem-phys.net/5/799/2005/acp-5-799-](http://www.atmos-chem-phys.net/5/799/2005/acp-5-799-2005.pdf)
1343 [2005.pdf](http://www.atmos-chem-phys.net/5/799/2005/acp-5-799-2005.pdf), last accessed 10 July 2014, 2005.

1344 Robinson, A. L., Donahue, N. M., Shrivastava, M. K., Weitkamp, E. A., Sage, A. M.,
1345 Grieshop, A. P., Lane, T. E., Jeffrey R. Pierce, J. R., and Pandis, S. N.: Rethinking

1346 organic aerosols: semivolatile emissions and photochemical aging, *Science*, 315, 1259
1347 – 1262, doi:10.1126/science.1133061, 2007.

1348 Saylor, R. D., Edgerton, E. S., and Hartsell, B. E.: Linear regression techniques for use in
1349 the EC tracer method of secondary organic aerosol estimation, *Atmos. Environ.*, 40,
1350 7546-7556, 2006.

1351 Schauer, J.J., Rogge, W.F., Hildemann, L.M., Mazurek, M.A., and Cass, G.R.: Source
1352 apportionment of airborne particulate matter using organic compounds as tracers,
1353 *Atmos. Environ.*, 30, 3837-3855, 1996.

1354 Shilling, J. E., Zaveri, R. A., Fast, J. D., Kleinman, L., Alexander, M. L., Canagaratna,
1355 M. R., Fortner, E., Hubbe, J. M., Jayne, J. T., Sedlacek, A., Setyan, A., Springston, S.,
1356 Worsnop, D. R., and Zhang, Q.: Enhanced SOA formation from mixed anthropogenic
1357 and biogenic emissions during the CARES campaign, *Atmos. Chem. Phys.*, 13, 2091-
1358 2113, doi:105194/acp-13-2091-2013, 2013.

1359 Southeast Atmosphere Study (SAS): https://www.eol.ucar.edu/field_projects/sas, last
1360 access 2 September 2014.

1361 Southern Oxidant and Aerosol Study (SOAS): <http://soas2013.rutgers.edu/>, last access 2
1362 September 2013.

1363 Surratt, J., Kroll, J., Kleindinst, T., Edney, E., Claeys, M., Sorooshian, A., Ng, N.,
1364 Offenberg, J., Lewandowski, M., Jaoui, M., Flagan, R., and Seinfeld, J.: Evidence for
1365 organosulfates in secondary organic aerosol, *Environ. Sci. Technol.*, 41, 517-527, 2007.

1366 Taylor, N., Collins, D., Spencer, C., Lowenthal, D., Zielenska, B., Samburova, V., and
1367 Kumar, N.: Measurement of ambient aerosol hydration state at Great Smoky Mountains
1368 National Park in the southeastern United States, *Atmos. Chem. Phys.*, 11, 12085-2011,
1369 doi:10.5194/acp-1112085-2011, 2011.

1370 Tang, I. N.: Chemical and size effects of hygroscopic aerosols on light scattering
1371 coefficients, *J. Geophys. Res.*, 101 (D14), 19245 – 19250, 1996.

1372 Tanner, R., Parkhurst, W., and McNichol, A.: Fossil sources of ambient aerosol carbon
1373 based on ¹⁴C measurements, *Aerosol Sci. Technol.*, 38, 133-139, 2004.

1374 Tombach, I.: Estimating Particle-Bound Water in Weighed Sulfate and Nitrate Particles
1375 Collected in the Southeast, report prepared for Southern Company, 2004.

1376 Turpin, B. J. and H.-J. Lim: Species contributions to PM_{2.5} mass concentrations:
1377 revisiting common assumptions for estimating organic mass, *Aerosol Sci. Technol.*, 25,
1378 602-610, 2001.

1379 U.S. EPA: SPECIATE website, <http://www.epa.gov/ttn/chief/software/speciate/> last
1380 access October 19, 2015.

1381 U.S. EPA: Research in Action: EPA Positive Matrix Factorization (PMF) Model,
1382 <http://www.epa.gov/heasd/research/pmf.html>, last access 12 November 2014.

1383 Varner, J. M., III, Gordon, D. R., Putz, F. E., and Hiers, J. K.: Restoring fire to long-
1384 unburned *Pinus palustris* ecosystems: novel fire effects and consequences for long-
1385 unburned ecosystems, *Restor. Ecol.*, 13, 536-544, 2005.

1386 Wade, D.D., Brock, B.L., Brose, P.H., Grace, J.B., Hoch, G.A., and Patterson, W.A.: Fire
1387 in eastern ecosystems, in: Brown & Smith, eds., *Wildland Fire in Ecosystems: Effects*
1388 *of Fire on Flora*, USDA Forest Service, Rocky Mountain Research Station, Gen. Tech.
1389 Rep. RMRS-42, Ogden, UT, 2000.

1390 Washenfelder, R., Attwood, A., Brock, C., Guo, H., Xu, L., Weber, R., Ng, N., Allen, H.,
1391 Ayres, B., Baumann, K., Cohen, R., Draper, C., Duffey, K., Edgerton, E., Fry, J.,
1392 Jiminez, J., Palm, B., Romer, P., Stone, E., Woodridge, P., and Brown, S.: Biomass
1393 burning dominates brown carbon absorption in the rural southeastern United States.
1394 *Geophys. Res. Lett.*, 42, doi:10.1002/2014GL062444, 2015.

1395 Watson, J. G., Chow, J. C., Chen, L.-W. A., Lowenthal, D. H., Fujita, E. M., Kuhns, H.
1396 D., Sodeman, D. A., Campbell, D. E., Moosmüller, H., and Zhu, D.Z.: Particulate
1397 emission factors for mobile fossil fuel and biomass combustion sources, *Sci. Total*
1398 *Environ.*, 409, 2384-2396, 2011.

1399 Watson, J., Chow, J. C., Lowenthal, D. H., Chen, L.-W. A., Shaw, S., Edgerton, E. S.,
1400 and Blanchard, C. L.: PM_{2.5} source apportionment with organic markers in the
1401 Southeastern Aerosol Research and Characterization (SEARCH) study, *J. Air Waste*
1402 *Manage. Assoc.*, 65, 1104 – 1118, doi:10.1080/10962247.2015.1063551, 2015.

1403 Weber, R.J., Sullivan, A.P., Peltier, R.E., Russell, A., Yan, B., Zheng, M., de Gouw, J.,
1404 Warneke, C., Brock, C., Holloway, J.S., Atlas, E.L., and Edgerton, E.: A study of
1405 secondary organic aerosol formation in the anthropogenic-influenced southeastern
1406 United States, *J. Geophys. Res.*, 112, D13302, 2007.

1407 Xu, L., Guo, H., Boyd, C. M., Klein, M., Bougiatioti, A., Cerully, K. M., Hite, J. R.,
1408 Isaacman-VanWertz, G., Kreisberg, N. M., Knote, C., Olson, K., Koss, A., Goldstein,
1409 A. H., Hering, S., de Gouw, J., Baumann, K., Lee, S-H., Nenes, A., Weber, R., and Ng,
1410 N. L.: Effects of anthropogenic emissions on aerosol formation from isoprene and
1411 monoterpenes in the southeastern United States, *P. Natl. Acad. Sci. USA*, 112, (1) 37-
1412 42, doi:10.1073/pnas.1417609112, 2015a.

1413 Xu, L. Suresh, S., Guo, H., Weber, R., and Ng, N.: Aerosol characterization over the
1414 southeastern United States using high-resolution aerosol mass spectrometry: spatial and
1415 seasonal variation of aerosol composition and sources with a focus on organic nitrates,
1416 *Atmos. Chem. Phys.*, 15, 7307-7336, 2015b.

1417 Yu, S., Bhave, P., Dennis, R., and Mathur, R.: Seasonal and regional variations of
1418 primary and secondary organic aerosols over the continental United States: semi-
1419 empirical estimates and model evaluation, *Environ. Sci. Technol.*, 41, 4690-4697, 2007.

1420 Zhang, X., Hecobian, A., Zheng, M., Frank, N., and Weber, R.: Biomass burning impact
1421 on PM_{2.5} over the southeastern US during 2007: integrating chemically speciated FRM
1422 filter measurements, MODIS fire counts and PMF analysis, *Atmos. Chem. Phys.*, 10,
1423 5839-6853, 2010.

1424 Zheng, M., Cass, G. R., Schauer, J. J., and Edgerton, E. S.: Source apportionment of
1425 PM_{2.5} in the southeastern United States using solvent-extractable organic compounds as
1426 tracers, *Environ. Sci. Technol.*, 36, 2361-2371, 2002.

1427 Zheng, M., Ke, L., Edgerton E. S., Schauer, J. J., Dong, M., and Russell, A. G.: Spatial
1428 distribution of carbonaceous aerosol in the southeastern United States using molecular
1429 markers and carbon isotope data, *J. Geophys. Res.*, 111, D10S06,
1430 doi:10.1029/2005JD006777, 2006.

1431

1432

1433

1434

1435

1436 Table 1. Five-year seasonal mean EC and OC concentrations at CTR and JST with mean
 1437 OC/EC.^a

Period ^b	CTR			JST		
	CTR EC	CTR OC	OC/EC	JST EC	JST OC	OC/EC
1999-03W	0.490 ± 0.025	2.615 ± 0.154	5.34	1.725 ± 0.068	4.801 ± 0.153	2.78
1999-03Sp	0.607 ± 0.030	3.411 ± 0.154	5.62	1.410 ± 0.037	4.465 ± 0.096	3.17
1999-03Su	0.537 ± 0.020	3.541 ± 0.100	6.59	1.439 ± 0.035	4.664 ± 0.090	3.24
1999-03A	0.684 ± 0.026	3.814 ± 0.145	5.58	1.808 ± 0.060	5.264 ± 0.150	2.91
2004-08W	0.538 ± 0.036	2.348 ± 0.167	4.37	1.319 ± 0.050	4.099 ± 0.125	3.11
2004-08Sp	0.556 ± 0.029	3.269 ± 0.199	5.88	1.173 ± 0.034	4.283 ± 0.135	3.65
2004-08Su	0.528 ± 0.030	3.267 ± 0.151	6.19	1.292 ± 0.032	4.114 ± 0.077	3.19
2004-08A	0.551 ± 0.024	2.850 ± 0.120	5.17	1.375 ± 0.049	3.852 ± 0.093	2.30
2009-13W	0.402 ± 0.027	2.066 ± 0.136	5.14	0.859 ± 0.060	2.828 ± 0.155	3.29
2009-13Sp	0.354 ± 0.018	2.243 ± 0.117	6.34	0.699 ± 0.039	2.774 ± 0.128	3.97
2009-13Su	0.357 ± 0.017	2.818 ± 0.112	7.89	0.723 ± 0.024	2.870 ± 0.095	3.97
2009-13A	0.437 ± 0.024	2.579 ± 0.105	6.31	0.926 ± 0.042	2.934 ± 0.110	3.05

1438 a. Uncertainties are one standard error of the means. OC/EC is computed as ratios of means.
 1439 Propagation of errors yields one standard error of OC/EC ranging from 0.30 to 0.49 for CTR (mean
 1440 0.41) and 0.10 to 0.29 for JST (mean 0.16).

1441 b. W = Dec, Jan, Feb; Sp = Mar, Apr, May; Su=Jun, Jul, Aug; A = Sep, Oct, Nov

1442

1443

1444

1445 Table 2. Species associated with each PCA factor (component). Component names are
 1446 keyed to the species. Three species are listed in decreasing order of association for
 1447 associations of 0.6 or greater (or -0.6 or smaller). Negative values indicate anti-
 1448 correlation. CO^x and SO₂^x are 1-hour daily maximum CO and SO₂, respectively. O₃^x is 8-
 1449 hour daily maximum O₃. PCA1, 2008 – 2013; PCA2, 1999 – 2013. N = number of days.

PCA	Site	N	Combustion	Crustal	Seasonal	SO ₂	SO ₄	Metals	Salt	Other
1	BHM	364	CO, NO _x , OC	Al, Si	NO ₃	SO ₂ ^x , SO ₂	NH ₄ , SO ₄	Zn, Cu, Fe	K	NO _z
1	CTR	383	EC, OC, CO	Si, Fe, Al	NH ₃	SO ₂ , SO ₂ ^x	SO ₄ , NH ₄	Cu, Zn	Na, Cl, Mg	
1	GFP	100	CO, CO ^x , NO _x	Si, Fe, Al	O ₃ ^x , NH ₃	SO ₂ , SO ₂ ^x	NH ₄ , SO ₄		Cl, Na, Mg	Ca
1	JST	516	CO, NO _x , EC	Si, Al, Fe	O ₃ ^x , NH ₃ , -NO ₃	SO ₂ ^x , SO ₂	NH ₄ , SO ₄		K, Cl, Mg	Na
1	OAK	100	CO ^x , CO	Fe, Al, Si	NH ₃ , O ₃ ^x	SO ₂ ^x , SO ₂	SO ₄ , NH ₄	NO _x , Cu, NO _z , Zn	Na, Cl, Mg	
1	OLF	327	NO _x , CO, EC	Si, Al, Fe	NH ₃ , O ₃ ^x	SO ₂ , SO ₂ ^x	SO ₄ , NH ₄	Cu	Na, Mg, Cl	
1	PNS	44	CO, NO _x , EC	Si, Al, Fe	O ₃ ^x	SO ₂ , SO ₂ ^x	NH ₄ , SO ₄		Na, Mg, Cl	
1	YRK	426	NO _x , NO ₃ , CO	Si, Fe, Al	O ₃ ^x , OC, EC	SO ₂ ^x , SO ₂	SO ₄ , NH ₄	Cu	Na, Cl, Mg	Zn
2	BHM	1513	CO, CO ^x , NO _x	Al, Si	O ₃ , O ₃ ^x , -NO ₃	SO ₂ ^x , SO ₂	NH ₄ , SO ₄	Zn, Cu, Fe		
2	CTR	1258	OC, EC, CO ^x	Si, Fe, Al	O ₃ ^x , O ₃	SO ₂ , NO _x , SO ₂ ^x	SO ₄ , NH ₄	Cu		
2	GFP	376	CO ^x , CO, NO _x	Si, Fe, Al	O ₃ , O ₃ ^x	SO ₂ ^x , SO ₂	NH ₄ , SO ₄	Cu, Zn		
2	JST	2593	CO, CO ^x , NO _x	Si, Al, Fe	NO ₃ , -O ₃ ^x , -O ₃	SO ₂ ^x , SO ₂	NH ₄ , SO ₄ , O ₃ ^x	Cu		
2	OAK	707	CO ^x , CO, EC	Si, Fe, Al	O ₃ , O ₃ ^x	SO ₂ ^x , SO ₂	SO ₄ , NH ₄	Cu, Zn		
2	OLF	948	CO ^x , CO, NO _x	Si, Fe, Al	O ₃ , O ₃ ^x	SO ₂ ^x , SO ₂	NH ₄ , SO ₄ , NO _z	Zn, Cu		
2	PNS	445	EC, CO, NO _x	Si, Al, Fe	O ₃ ^x , O ₃ , SO ₄ , NH ₄	SO ₂ ^x , SO ₂		Cu		NO _z
2	YRK	1435	CO ^x , NO _x , NO ₃	Si, Fe, Al	O ₃ ^x , SO ₄ , O ₃ , NH ₄	SO ₂ ^x , SO ₂		Cu		Zn

1450

1451

1452

1453 Table 3. Mean OC concentrations associated with components identified by PCA1 (2008
 1454 – 2013) and PCA2 (1999 – 2013). NS = not statistically significant, NA = not applicable
 1455 (component not present in PCA). Units are $\mu\text{g m}^{-3}$. Standard errors of the means ranged
 1456 from 0.003 to 0.09 $\mu\text{g m}^{-3}$ (up to 0.25 $\mu\text{g m}^{-3}$ for PNS PCA1).

PCA	Site	N	Combustion	Crustal	Seasonal	SO ₂	SO ₄	Metals	Salt	Other
1	BHM	364	1.36	0.09	0.40	0.35	0.45	0.15	0.14	0.10
1	CTR	383	1.28	0.26	0.56	NS	0.33	NS	NS	NA
1	GFP	100	0.95	NS	0.45	0.15	0.25	NS	-0.41	0.62
1	JST	516	1.09	0.16	0.49	0.07	0.27	NA	0.64	0.11
1	OAK	100	0.40	NS	0.50	0.37	0.53	0.32	-0.27	NA
1	OLF	327	0.74	-0.08 ^a	0.52	0.16	0.27	NS	-0.09 ^a	NA
1	PNS	44	1.95	NS	0.33	NS	0.56	NA	-0.63	NA
1	YRK	426	0.14	0.14	1.09	NS	0.26	0.16	0.15	0.47
2	BHM	1513	1.60	0.19	0.47	0.38	0.57	0.48	NA	NA
2	CTR	1258	1.50	0.12	0.69	NS	0.66	NS	NA	NA
2	GFP	376	0.72	0.14	0.37	0.21	0.50	0.25	NA	NA
2	JST	2593	2.58	0.32	0.06 ^b	NS	1.01 ^b	0.13	NA	NA
2	OAK	707	1.50	NS	0.47	NS	0.59	NS	NA	NA
2	OLF	948	0.81	-0.06 ^a	0.25	0.09	1.02	0.20	NA	NA
2	PNS	445	1.55	NS	0.45 ^c	0.17	NA	NS	NA	0.36
2	YRK	1435	0.76	0.20	1.40 ^c	0.05	NA	0.39	NA	0.29

1457 a. OLF PCA1 and PCA2 crustal and PCA1 salt OC mean concentrations are negative due to inverse
 1458 associations of OC with crustal and salt components at OLF (Tables S7 and S12).

1459 b. JST PCA2 seasonal OC is associated with NO₃; JST PCA2 SO₄ component includes OC associated
 1460 with O₃ (Table 2).

1461 c. PNS and YRK PCA2 seasonal components include OC associated with SO₄ (Table 2).

1462

1463 Table 4. Ranges of mean OC concentrations associated with each PCA component. The
 1464 time period is 2009 – 2013. For each site, multiple methods were compared using a
 1465 common set of days. For CTR (6 methods), both the standard deviation and one-half the
 1466 range of component mean concentrations are shown. For JST (3 methods), one-half the
 1467 range of component mean concentrations is shown. For YRK (2 PCA methods), ranges
 1468 are shown. YRK ranges are smaller than ranges for CTR and JST because no PMF
 1469 analyses were carried out for YRK. The larger ranges for CTR and JST compared with
 1470 YRK reflect the larger differences between PCA and PMF.

Component	CTR ^a				JST ^b		YRK ^c	
	Range/2 ($\mu\text{g m}^{-3}$)	Range/2 (% of mean)	Std Dev ($\mu\text{g m}^{-3}$)	Std Dev (% of mean)	Range/2 ($\mu\text{g m}^{-3}$)	Range/2 (% of mean)	Range ($\mu\text{g m}^{-3}$)	Range (% of mean)
Combustion	0.44	18	0.30	12	0.34	12	0.34	14
Crustal	0.09	4	0.07	3	0.11	4	0.09	4
Sulfate	0.15	6	0.11	4	0.19	7	0.26	11
Seasonal	0.36	15	0.25	10	0.43	15	0.12	5
SO ₂					0.03	1	0.03	1
Metals					0.07	2	0.04	2
Salt					0.33	12	0.16	7
Other					0.05	2	0.16	7

1471 a. Mean OC = 2.43 $\mu\text{g m}^{-3}$, n = 383 days, number of methods = 6 (4 PCA, 2 PMF)

1472 b. Mean OC = 2.85 $\mu\text{g m}^{-3}$, n = 398 days, number of methods = 3 (2 PCA, 1 PMF)

1473 c. Mean OC = 2.40 $\mu\text{g m}^{-3}$, n = 426 days, number of methods = 2 (2 PCA)

1474

1475

1476 Table 5. Mean OC concentrations determined for the period 2008 – 2013 using four
 1477 analytical approaches: (1) multivariate regression (“POC” and “SOC”, Blanchard et al.,
 1478 2008), (2) calculation of OC_{bb} from K_{bb} tracer, (3) PCA and PMF analysis, and (4)
 1479 CMB receptor-modeling (Blanchard et al., 2013, updated). Row indentations indicate
 1480 subcategories. Units are $\mu\text{g m}^{-3}$ unless specified as %.

Component	BHM	CTR	GFP	JST	OAK	OLF	PNS	YRK	Unc^a
OC (mean measured)	2.91	2.41	1.91	2.86	1.84	1.81	2.06	2.33	0.05
“POC” ^b	1.85	1.78	1.40	2.12	1.35	1.36	1.57	1.61	25%
OC _{bb}	1.58	1.60	1.64	1.40	1.63	1.62	1.77	1.37	2X
PCA1 Combustion	1.36	1.28	0.95	1.07	0.40	0.85	1.95	0.13	0.3 - 0.6
PCA2 Combustion	1.09	1.47	0.45	1.83	0.87	0.60	1.26	0.49	0.3 - 0.6
PMF Combustion	NA	1.03	NA	1.22	NA	NA	NA	NA	0.3 - 0.6
CMB Combustion Total	2.54	1.52	1.33	2.16	1.42	1.47	1.89	1.49	0.87
CMB Area Sources	2.01	1.44	1.15	1.50	1.35	1.34	1.68	1.35	20 - 33%
CMB Mobile Diesel	0.20	0.02	0.05	0.27	0.01	0.05	0.04	0.04	13 - 31%
CMB Mobile Gas	0.29	0.03	0.10	0.34	0.03	0.05	0.15	0.06	17 - 41%
CMB Point Sources	0.05	0.02	0.02	0.05	0.02	0.03	0.03	0.04	5 - 6%
PCA1 Crustal	0.09	0.26	0.00	0.15	0.00	-0.14	0.00	0.14	0.09 - 0.11
PCA2 Crustal	0.20	0.12	0.17	0.35	0.00	-0.06	0.00	0.22	0.09 - 0.11
PMF Crustal	NA	0.09	NA	0.17	NA	NA	NA	NA	0.09 - 0.11
CMB Dust	0.09	0.02	0.04	0.03	0.03	0.02	0.04	0.01	9 - 22%
“SOC” ^b	1.10	0.66	0.56	0.75	0.48	0.48	0.50	0.77	25%
PCA1 Seasonal+Sulfate	0.85	0.90	0.70	0.76	1.03	1.00	0.90	1.26	0.3 - 0.5
PCA1 Seasonal	0.39	0.57	0.45	0.49	0.50	0.71	0.33	1.00	0.1 - 0.4
PCA1 Sulfate	0.45	0.33	0.25	0.27	0.53	0.29	0.56	0.26	0.2 - 0.3
PCA2 Seasonal+Sulfate	0.92	0.95	0.81	0.76	0.99	0.93	0.41	0.86	0.3 - 0.5
PCA2 Seasonal	0.51	0.53	0.40	0.05	0.40	0.28	0.41	0.86	0.1 - 0.4
PCA2 Sulfate	0.42	0.42	0.41	0.71	0.58	0.65	0.00	0.00	0.2 - 0.3
PMF Seasonal+Sulfate	NA	0.77	NA	1.32	NA	NA	NA	NA	0.3 - 0.5
PMF Seasonal	NA	0.49	NA	0.86	NA	NA	NA	NA	0.1 - 0.4
PMF Sulfate	NA	0.28	NA	0.46	NA	NA	NA	NA	0.2 - 0.3
N days (2008 - 2013, varies by analysis)	366 - 1313	383 - 606	100 -280	443 - 787	100 - 206	327 - 598	44 - 162	426 - 585	

1481 a. Uncertainty for mean measured OC is 1 standard error of the mean. Uncertainties
 1482 for PCA and PMF are taken from Section 3.5.3. Uncertainty for CMB combustion
 1483 total is RMSE across sites and years, where error is defined as the difference
 1484 between predicted and observed concentrations. Uncertainty for CMB
 1485 components is based on uncertainties in inputs and across alternative versions of
 1486 the model expressed as 1-sigma % of prediction (Blanchard et al., 2013).
 1487 b. “POC” is the sum of OC associated with EC, CO, and K_{bb}. “SOC” is the sum of
 1488 OC associated with O₃, and SO₄. “POC” is used as a fitting species in CMB.

1489

1490 **Figure Captions**

1491

1492 Figure 1. Seasonal mean EC and OC concentrations at CTR and JST. All correlations
1493 among the four time series are statistically significant ($p < 0.05$): CTR EC and OC, $r =$
1494 0.68 (95% CI $0.52 - 0.80$); JST EC and OC, $r = 0.87$ (95% CI $0.79 - 0.92$); CTR EC and
1495 JST EC, $r = 0.76$ (95% CI $0.62 - 0.85$); CTR OC and JST OC, $r = 0.68$ (95% CI $0.51 -$
1496 0.79).

1497

1498 Figure 2. Statistical distributions of the ratio OM^*/OC computed for daily-average
1499 measurements at SEARCH sites, 2009 – 2013. The distributions show the 10th, 25th, 50th,
1500 75th, and 90th percentiles. OM^* is the sum of measured OC and the computed difference
1501 of $PM_{2.5}$ mass minus the sum of measured species concentrations.

1502

1503 Figure 3. Monthly-average measured OC (solid blue line) and computed biomass burning
1504 OCbb (solid green line with surrounding shaded area indicating estimated uncertainty) at
1505 CTR. Trends in OC (dashed blue line) are statistically significant ($p < 0.05$); trends in
1506 OCbb (dashed green line) are not statistically significant.

1507

1508 Figure 4. Trends in source contributions to OC at CTR and JST determined from PCA2
1509 for 1999 - 2013.

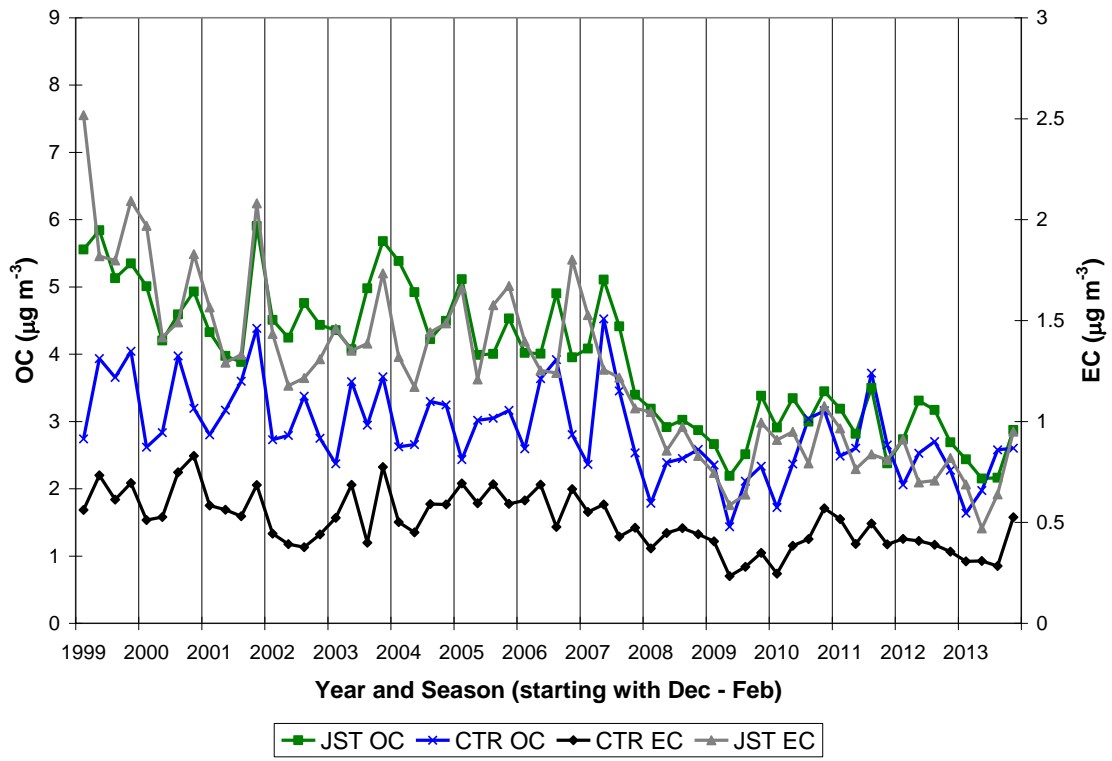
1510

1511

1512

1513

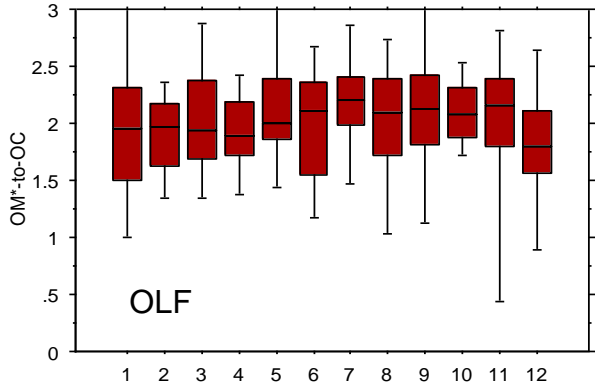
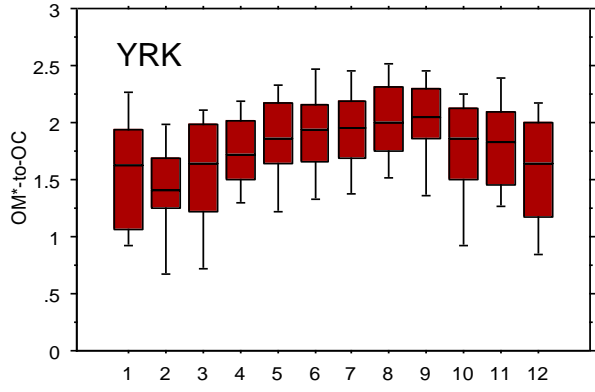
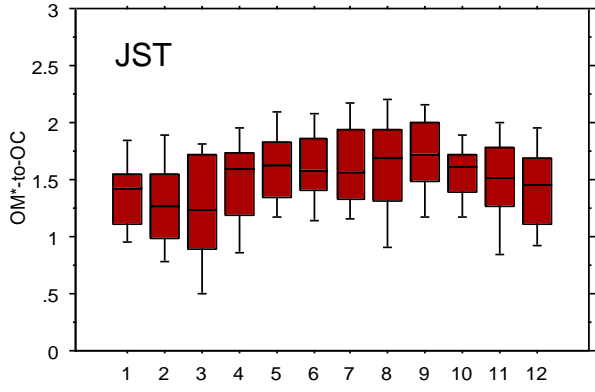
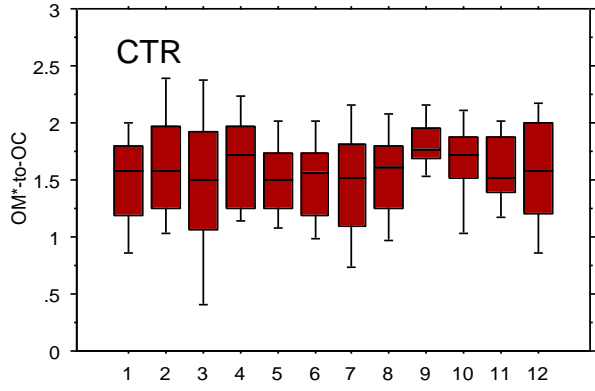
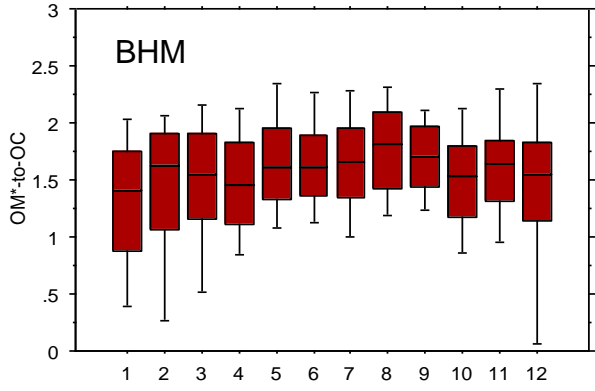
1514



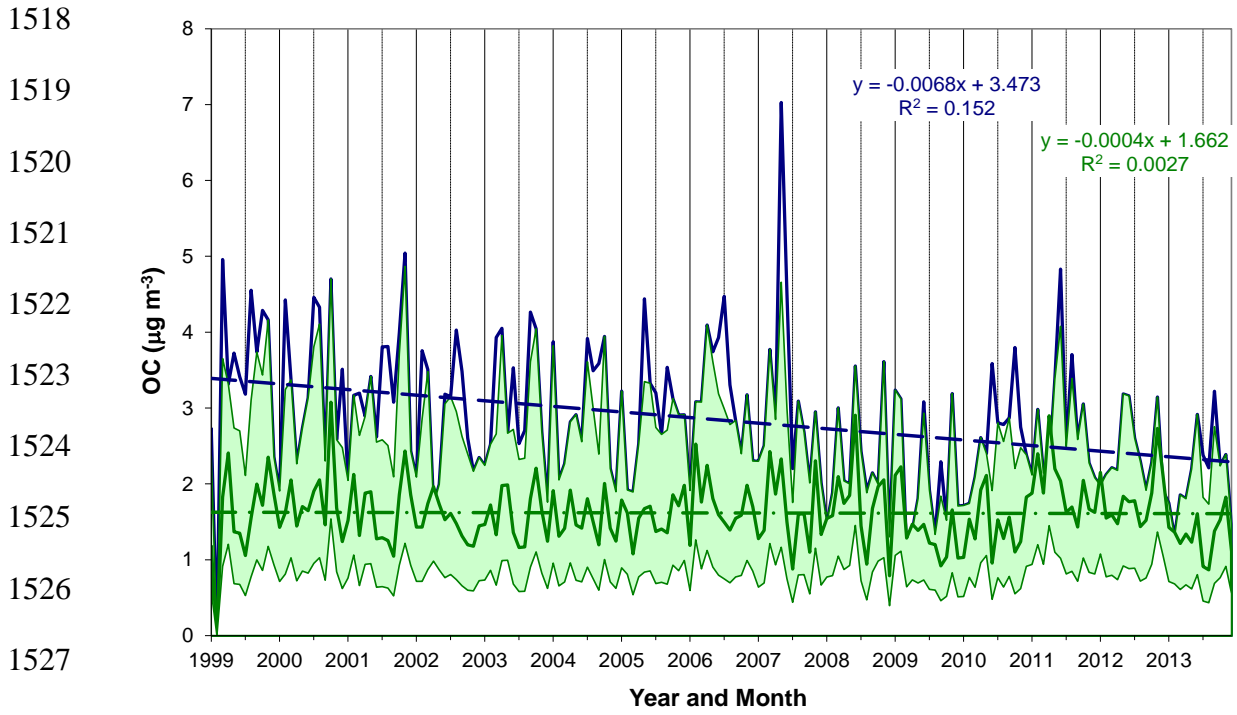
1515

1516

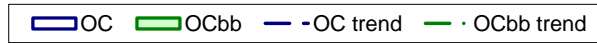
1517



Month



1518
 1519
 1520
 1521
 1522
 1523
 1524
 1525
 1526
 1527
 1528
 1529
 1530
 1531



1532
 1533
 1534
 1535
 1536

